

Nonlinear Bosonization and Refermionization in One Dimension with the Keldysh Functional Integral

Filippo Bovo

12th August 2021

School of Physics and Astronomy, University of Birmingham, Edgbaston, Birmingham, B15 2TT, UK.

Abstract

We develop a self-contained approach to bosonization and refermionization using the Keldysh functional integral. Starting from fermionic particles, we bosonize the system and obtain a description in terms of the Tomonaga-Luttinger liquid, with, in addition, an infinite series of interaction terms arising from the curvature of the fermionic particle spectrum. We explicitly calculate the leading interaction term and check its consistency with a different approach based on the Matsubara framework, within which we calculate the second leading interaction term, as well. Moreover, we bosonize weakly and strongly interacting bosonic particles, and, finally, refermionize interacting phonons into non-interacting fermionic quasiparticles. The work culminates in a map between bosonic and fermionic particles and effective bosonic and fermionic excitations, representing phonons and fermionic quasiparticles.

1 Introduction

Quantum systems in one dimension have been studied intensively with regard to their static or equilibrium properties. Equilibrium properties are associated with low energies, and one of the most important results for quantum systems in one dimension is that their low-energy theory can be expressed in terms of non-interacting phonons, even though the particles constituting the system are interacting. This result is known as bosonization [1, 2, 3, 4, 5, 6], and the phenomenology behind its success relies on this fact: particles moving in one dimension cannot avoid each other as would be possible in higher dimensions. As a consequence, any amount of interaction between particles leads to a behaviour where each particle pushes the next one in line in a sequence that leads to a density wave, that is, a phonon.

Despite the fact that non-interacting phonons describe particularly well one-dimensional systems in equilibrium, they are not sufficient for a proper description of dynamical or non-equilibrium properties, where higher energies become important. At zero temperatures, to capture the dynamics it is sufficient to couple a single mobile impurity, representing higher energies, to phonons, representing low energies [6, 7]. Instead, finite temperatures require a thermodynamical number of mobile impurities [8].

The passage from static to dynamic properties and from zero to finite temperatures requires a robust theoretical framework in order to capture the properties of these systems. At zero temperature, the real time many-body quantum field theory is a successful tool both for static and dynamic properties [7]. At finite temperatures, the imaginary time Matsubara formalism is suitable for static properties [6] and the Keldysh formalism is the natural candidate for dynamic properties [9]. Because of the recent interest in the dynamics of one-dimensional quantum systems at finite temperatures [7], in this work we derive a self-contained framework for these systems within the Keldysh formalism¹.

We start with a phenomenological derivation of the hydrodynamic theory of one-dimensional systems, describing low-energy excitations in terms of phonons. After that, we turn to study fermionic particles, starting from an overview of the spectrum of excitations of free fermions to introduce important concepts to which we will refer in the rest of the work. Using these concepts, we bosonize a system of interacting fermions and obtain an equivalent description in terms of interacting phonons. We proceed by evaluating the leading contribution, corresponding to the Tomonaga-Luttinger liquid. Extending this result, we express the system as the sum of the Tomonaga-Luttinger liquid, representing non-interacting phonons, and an infinite series of terms, induced by the curvature of the fermionic spectrum, describing interactions between an arbitrary number of phonons. We

¹We will use Keldysh formalism and notation developed in Ref. [9].

explicitly calculate the low-energy asymptotic expression of the leading interaction term, representing the interaction between three phonons, and check the consistency of this result in the Appendix using the Matsubara formalism. In addition, in the Appendix, we derive the the low-energy asymptotic expression of the next leading interaction term. Then we turn to a system of bosonic particles with contact interactions and, in the cases of weak and strong interactions, derive a description of their low-energy excitations in terms of phonons. We conclude the work by refermionizing the phononic systems obtained starting from fermions or bosons to obtain a description of the low-energy excitations in terms of free fermionic quasiparticles. Finally, we gather the results into a map that translates between bosonic and fermionic particles and effective bosonic and fermionic excitations, representing phonons and fermionic quasiparticles.

2 Hydrodynamics

In one dimension, systems of bosonic and fermionic particles behave differently than in higher dimensions, as particles constrained to move on a line cannot avoid each other. As a consequence, fermions, even in absence of interactions, cannot go past each other because of the Pauli exclusion principle and, similarly, for bosons with local repulsive interactions [6, 5]. These systems are dominated by collisions and, for times longer than the time between two consecutive collisions, are in a hydrodynamic regime. Since longer times translate into lower energies, at low enough energies we expect these systems to be described by the hydrodynamic Hamiltonian of a liquid [10],

$$\hat{H} = \int dx \left[\frac{1}{2} m \hat{n}(x) \hat{v}(x)^2 + e_0[\hat{n}] - \mu \hat{n}(x) \right],$$

where $\hat{n}(x)$ and $\hat{v}(x)$ are the density and velocity operators of the liquid, m and $e_0[\hat{n}]$ are the mass and the ground state energy per unit length and μ is the chemical potential. The first and second terms in the square brackets are respectively the kinetic and internal energies of the liquid.

The ground state of the liquid corresponds to $\hat{v} = 0$ and $\hat{n} = n$, where n is the constant homogeneous density determined by $e'_0[n] = \mu$ and the prime symbol, $'$, denotes derivative with respect to the argument. The low-energy physics is associated with small variations of velocity, \hat{v} , and density, $\hat{\rho}$, over the ground state values, $\hat{v} = 0$ and $\hat{n} = n$. Expressing the density as $\hat{n} = n + \hat{\rho}$, the Hamiltonian becomes,

$$\hat{H} = \int dx \left[\frac{1}{2} m (n + \hat{\rho}) \hat{v}^2 + e_0(n + \hat{\rho}) - \mu (n + \hat{\rho}) \right],$$

and expanding over the small variations, $\hat{\rho}$ and \hat{v} , we have,

$$\hat{H} \approx L [e_0(n) - \mu n] + \int dx \left[\frac{1}{2} \left(mn\hat{v}^2 + \frac{1}{\kappa n^2} \hat{\rho}^2 \right) + \frac{m}{2} \hat{\rho}\hat{v}^2 + \frac{\alpha}{6} \hat{\rho}^3 \right], \quad (1)$$

where $\kappa = 1/n^2 e_0''[n]$ is the compressibility of the liquid [11], $\alpha = e_0'''[n]$ and we neglected higher order terms. It is common to express the hydrodynamic Hamiltonian in terms of the phase fields $\theta(x, t)$ and $\phi(x, t)$, related to density and velocity as [4, 5, 6, 7],²

$$\begin{aligned} \hat{\rho}(x, t) &= \frac{1}{\pi} \partial_x \hat{\theta}(x, t), \\ \hat{v}(x, t) &= \frac{1}{m} \partial_x \hat{\phi}(x, t). \end{aligned} \quad (2)$$

Substituting Eqs. (2) in Hamiltonian (1) we obtain,

$$\begin{aligned} \hat{H} &= L [e_0(n) - \mu n] \\ &+ \int dx \left[\frac{c}{2\pi} \left(K(\partial_x \hat{\phi})^2 + \frac{1}{K} (\partial_x \hat{\theta})^2 \right) + \frac{1}{2\pi m} \partial_x \hat{\theta} (\partial_x \hat{\phi})^2 + \frac{\alpha}{6\pi^3} (\partial_x \hat{\theta})^3 \right], \end{aligned} \quad (3)$$

where we defined the speed of sound, c , and the Luttinger parameter, K , as [6],

$$\begin{aligned} c &= \frac{1}{\sqrt{\kappa m n}}, \\ \frac{K}{\pi} &= \sqrt{\frac{\kappa n^3}{m}}. \end{aligned} \quad (4)$$

The quadratic part of Eq. (3), is the Tomonaga-Luttinger liquid Hamiltonian describing linear waves in one dimension [6, 1, 2, 4, 5]. The cubic terms are the non-linear part of the Hamiltonian and are useful to the dynamics of one-dimensional systems, as we will see later. In this work, we will see how the low-energy physics of bosons and fermions with local repulsive interactions in one dimension is described by hydrodynamics Hamiltonian (3) and how to map it into an effective theory of free fermionic quasiparticles.

3 Fermion hydrodynamics

In this section we derive the hydrodynamic theory for interacting fermions. Since hydrodynamics is a theory of low-energy excitations, it is instructive to study the low-energy excitations of free fermions at zero and finite temperatures. At zero temperature, $T = 0$, fermions occupy all the states below the Fermi surface, as shown by the grey region in

²Here we follow the convention of Refs. [4, 5]. The convention of Refs. [6, 7] is obtained by the substitutions $\phi \rightarrow \theta$ and $\theta \rightarrow -\phi$ in our equations.

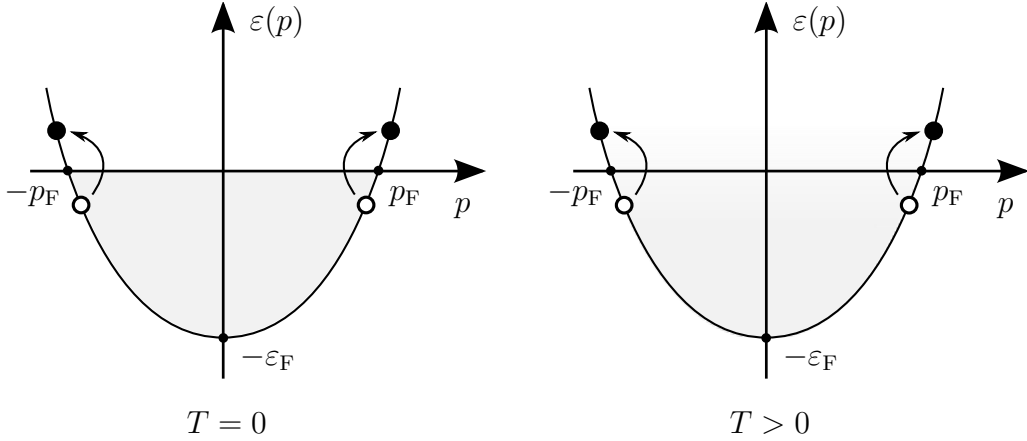


Figure 1: Occupation of states for free fermions at zero temperature, $T = 0$, and finite temperature, $T > 0$. The Fermi sea is represented by the grey regions and the Fermi surface is constituted by two separate points, $p = \pm p_F$. The temperature leads to a smearing of the average occupation of states around the Fermi surface. The circles and arrows represent particle-hole excitations.

Fig. 1-left, forming the Fermi sea. The Fermi surface in one dimension is constituted by two separate points in momentum space, $p = \pm p_F$, a central fact for one dimensional hydrodynamics, as we will see soon. Fermions inside the Fermi sea are frozen due to the Pauli exclusion principle. However, they can jump across the Fermi points to the unfilled region above, as shown by the arrows in Fig. 1-left. This process is referred to as particle-hole excitation. The height of the jump is the energy of the excitation and it becomes clear that low-energy particle-hole excitations are fermions just below a Fermi point jumping slightly above it. As a consequence, low-energy particle-hole excitations must cross the Fermi points and remain close to them. At temperatures much smaller than the Fermi energy, $T \ll \varepsilon_F = \frac{p_F^2}{2m}$, where m is the mass of fermions, the average occupation of the states is smeared around the Fermi points, as shown by the grey region in Fig. 1-right. However, the above argument still holds. Then, given that particle-hole excitations can be arbitrarily close to the Fermi surface, they constitute the lowest energy excitations of the system, suggesting that they could be good candidates for the hydrodynamical description.

To check this intuitive picture, we study the spectrum of particle-hole excitations. For the moment, we use the operator formalism of second quantisation, as it leads to a better insight. Although the particle-hole excitation spectrum of free fermions is known [7], it is useful to review its calculation in order to build some intuition. We start from the zero temperature case and later extend the results to low temperatures. The spectrum of particle-hole excitations can be studied using the dynamical structure factor, that gives the probability per unit time to excite a density fluctuation of momentum q and energy ω

by an external source. This quantity is accessible through Bragg spectroscopy [12] and was recently measured for an array of one-dimensional Bose gases [13]. The dynamical structure factor is defined as the Fourier transform of the density-density correlation [14, 7],

$$S(q, \omega) = \int_0^L dx \int_{-\infty}^{\infty} dt \langle \hat{n}(x, t) \hat{n}(0, 0) \rangle e^{-iqx + i\omega t}, \quad (5)$$

where $\hat{n}(x, t)$ is the density operator, L is the system size and $\langle \dots \rangle \equiv \langle 0 | \dots | 0 \rangle$ denotes the expectation value over the ground state, $|0\rangle$. Inserting the completeness relation $\sum_j |j\rangle \langle j| = 1$, where j labels the energy eigenstates, between the densities in Eq. (5), we obtain,

$$S(q, \omega) = \int_0^L dx \int_{-\infty}^{\infty} dt \sum_j \langle 0 | \hat{n}(x, t) | j \rangle \langle j | \hat{n}(0, 0) | 0 \rangle e^{-iqx + i\omega t}.$$

Making the time dependence of the density explicit, $\hat{n}(x, t) = e^{i\hat{H}t} \hat{n}(x) e^{-i\hat{H}t}$, we have,

$$S(q, \omega) = \int_0^L dx \int_{-\infty}^{\infty} dt \sum_j e^{-i(E_j - E_0)t} \langle 0 | \hat{n}(x) | j \rangle \langle j | \hat{n}(0) | 0 \rangle e^{-iqx + i\omega t},$$

where E_j is the energy of the state $|j\rangle$ and E_0 is the energy of the ground state. Integrating over time we find,

$$S(q, \omega) = 2\pi \int_0^L dx \sum_j \langle 0 | \hat{n}(x) | j \rangle \langle j | \hat{n}(0) | 0 \rangle e^{-iqx} \delta(\omega - E_j + E_0).$$

In terms of the Fourier transform of the fermionic creation and annihilation operators of momentum k , \hat{c}_k^\dagger and \hat{c}_k , the density reads $\hat{n}(x) = \frac{1}{L} \sum_q \hat{n}_q e^{iqx} = \frac{1}{L} \sum_{q,k} \hat{c}_{k-q}^\dagger \hat{c}_k e^{iqx}$ and the dynamical structure factor becomes,

$$S(q, \omega) = \frac{2\pi}{L} \sum_j \sum_{q', k, k'} \langle 0 | \hat{c}_{k-q}^\dagger \hat{c}_k | j \rangle \langle j | \hat{c}_{k'-q'}^\dagger \hat{c}_{k'} | 0 \rangle \delta(\omega - E_j + E_0). \quad (6)$$

Here, $\hat{c}_{k+q}^\dagger \hat{c}_k | 0 \rangle$ is the ground state plus a particle excited from momentum k to momentum $k+q$, as pictured in Fig. 2, that is, a particle-hole excitation. Due to the orthogonality of these excited states, the only non-zero contribution comes from $|j\rangle = \hat{c}_{k+q}^\dagger \hat{c}_k | 0 \rangle =$

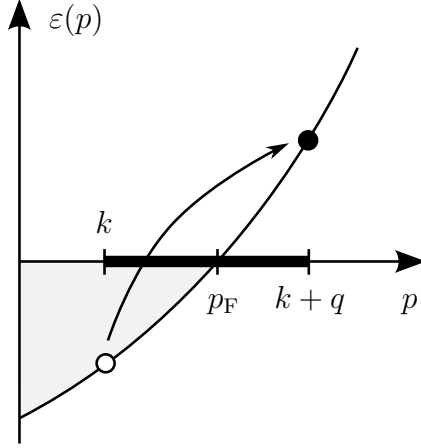


Figure 2: Particle-hole excitation close to the right Fermi point, p_F , given by a fermion with momentum k below the Fermi point excited to a state with momentum $k + q$ above the Fermi point. The momentum of the particle-hole excitation, q , is represented by the thick line. The dashed line is the linearisation of the spectrum around the Fermi point.

$\hat{c}_{k'+q}^\dagger \hat{c}_{k'} |0\rangle$, which also imposes $q = q'$ and $k = k'$. Then,

$$\begin{aligned} S(q, \omega) &= \frac{2\pi}{L} \sum_k \left| \langle 0 | \hat{c}_k^\dagger \hat{c}_{k+q} \hat{c}_{k+q}^\dagger \hat{c}_k | 0 \rangle \right|^2 \delta \left(\omega - \frac{q(q+2k)}{2m} \right) \\ &\approx \frac{m}{q} \int dk \left| \langle 0 | \hat{c}_k^\dagger \hat{c}_{k+q} \hat{c}_{k+q}^\dagger \hat{c}_k | 0 \rangle \right|^2 \delta \left(k - \frac{m\omega}{q} + \frac{q}{2} \right), \end{aligned}$$

where we approximated the sum by the integral and we used the fact that the energy of the ground state plus a particle excited from momentum k to momentum $k - q$ is,

$$E_j = E_0 + \frac{(k+q)^2}{2m} - \frac{k^2}{2m} = E_0 + \frac{q(q+2k)}{2m}.$$

In order for $c_{k+q}^\dagger c_k |0\rangle$ to be different from zero, because of the Pauli exclusion principle, c_k has to annihilate a particle inside the Fermi sea, that is, $|k| \leq k_F$, and c_{k+q}^\dagger has to create a particle outside the Fermi sea, that is, $|k+q| > k_F$. In other words, in the case of the right Fermi point, p_F , the momentum q of the particle-hole excitation is represented by the thick line in Fig. 2 that can move left or right but has to be pinned to the Fermi point. Considering only positive q , for $q \leq 2k_F$ the restriction on k becomes $k_F - q < k \leq k_F$ and the result is symmetric for negative q . Finally, integrating over k we obtain,

$$\begin{aligned} S(q, \omega) &= \frac{m}{q} \theta(\omega - \omega_-(q)) \theta(\omega_+(q) - \omega), \\ \omega_\pm(q) &= v_F q \pm \frac{q^2}{2m}, \end{aligned} \tag{7}$$

where $v_F = p_F/m$ is the Fermi velocity. The dynamical structure factor at zero temperature

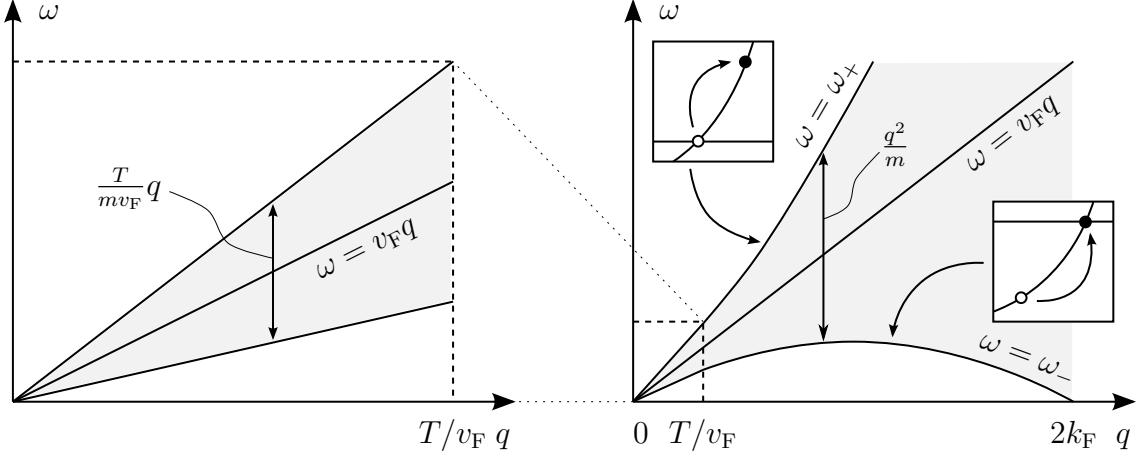


Figure 3: Dynamical structure factor, $S(q, \omega)$, of free fermions at a low temperature, $T \ll \varepsilon_F$. For $q \gg T/v_F$, $S(q, \omega)$ is given by the zero temperature result (7) and the grey colour represents the region where $S(q, \omega)$ is non-zero. The grey region is centred around $\omega = v_F q$ and is bounded above and below by $\omega = \omega_+(q)$ and $\omega = \omega_-(q)$, the energies corresponding to the extremal particle-hole excitations shown in the insets. For $q \ll T/v_F$, $S(q, \omega)$ is given by the small temperature result (9) and the grey colour represents qualitatively the width (10) of bell-shaped distribution centred around $\omega = v_F q$. The small temperature result is magnified in the right picture.

as a function of ω is a box centred around $v_F q$, of height m/q and width,

$$\delta\omega(q) = \omega_+(q) - \omega_-(q) = \frac{q^2}{m}. \quad (8)$$

Particle-hole excitations with momentum q and energy ω are present in the system where the dynamical structure factor is non-zero, that is, the grey region in Fig. 3-right (ignore $q \ll T/v_F$ for the moment). For each momentum, the dynamical structure factor is bound in energy above and below. The upper bound, $\omega = \omega_+(q)$, corresponds to a particle picked from the Fermi surface, k_F , and moved to $k_F + q$ and the lower bound, $\omega = \omega_-(q)$, corresponds to a particle picked from $k_F - q$ and moved to the Fermi surface, k_F , as shown in the insets of Fig. 3-right. Higher and lower bounds correspond to the thick line pinned to the Fermi surface in Fig. 2 moved completely to the right or left. Moving the thick line from right to left creates all the intermediate particle-hole excitations between higher and lower bounds, the grey region in Fig. 3. The peculiarity of one-dimensional systems is the absence of low-energy excitations away from $q = 0$ and $q = 2k_F$. This absence is related to the presence of the lower bound, which in turn is related to the Fermi surface in one dimension consisting of just two separate points. In higher dimensions, Fermi surfaces are continuous, for example, a circle in two dimensions, allowing one to play with angles to create excitations with arbitrary low energy for any momentum [6].

Now, we have a look at how the result is modified by the temperature. At temperatures

smaller than the Fermi energy, $T \ll \varepsilon_F$, the average over the ground state in Eq. (5) is replaced by the thermal average $\sum_i e^{-E_i/T} \langle i | \dots | i \rangle$, and for $q \ll T/v_F$ the dynamical structure factor becomes,³

$$S(q, \omega) = \frac{m}{q} n_F \left(v_F \frac{2m(\omega - v_F q) - q^2}{2q} \right) n_F \left(v_F \frac{-2m(\omega - v_F q) - q^2}{2q} \right) \quad (9)$$

$$\approx \frac{m}{4q} \frac{1}{\cosh^2 \left(\frac{mv_F}{2Tq} (\omega - v_F q) \right)}.$$

The procedure to obtain this result is similar to that at zero temperature just seen and has been omitted. As a function of ω , the dynamical structure factor has the shape of a bell centred around $\omega = v_F q$, of height $m/4q$ and width linear in q ,

$$\delta\omega_T(q) \sim \frac{T}{mv_F} q \quad (10)$$

The width at finite temperatures is equal to the one at zero temperature, Eq. (8), with one power of q replaced by the thermal momentum, T/v_F . The width of the dynamical structure factor is represented by the grey region in Fig. 3-left. The thermal momentum scale, T/v_F , separates a thermal region for $q \ll T/v_F$ from a quantum region for $q \gg T/v_F$ as shown in 3-left. The important observation is that both at zero and finite temperature the widths $\delta\omega(q)$ and $\delta\omega_T(q)$ are small compared to the mean value $v_F q$ in the small momentum and small energy limits, $q \ll k_F$, $\omega \ll \varepsilon_F$ and $T \ll \varepsilon_F$. Referring to the zero temperature dynamical structure factor in Fig. 3, it means that the excitations are centred around the line $\omega = v_F q$. In turn, this means that in this limit excitations have approximately fixed velocity v_F , like the speed of sound, c , of hydrodynamic wave excitation in Eq. (4). Therefore, we have an intuitive link between low-energy fermions and hydrodynamics. In the next two subsections we will see how the physics of low-energy excitations around the Fermi points leads to the hydrodynamic theory with speed of sound $c = v_F$ for free fermions and a modified speed of sound in presence of interactions.

3.1 Bosonization

We are ready to derive the hydrodynamic theory for interacting fermions, a procedure known as bosonization [6, 7]. Bosonization of interacting fermions was first derived by Haldane using the operator formalism of second quantisation [4, 5]. Complementary to the operator approach, a functional integral approach was suggested in Ref. [15], elaborated in

³Note that to satisfy the f -sum rule, $\int d\omega \omega S(q, \omega) \propto q^2/2m$, (see e.g., Ref. [14]), one needs to consider the full expression, the first line of Eq. (9). This is because the full expression correctly accounts for the detailed balance at negative ω .

Ref. [16] and presented in a clear picture in Refs. [17, 18, 19]. This approach is known as functional bosonization and relies on the Hubbard-Stratonovich transformations. All these approaches are based on equilibrium physics and an extension to non-equilibrium was obtained in Ref. [20] using the Keldysh technique. An appealing aspect of bosonization is that the initial theory of interacting fermions is reformulated as a non-interacting theory that is completely solvable. However, the non-interacting theory is a low-energy approximation to which refinements can be added. One of such refinement is the inclusion of non-linear corrections. A non-linear correction was derived in Ref. [4] using the operator formalism and the assumption that the excitations of the system are created above the ground state. Here we will derive the functional bosonization using the Keldysh technique and, in the spirit of Ref. [21], a double Hubbard-Stratonovich transformation approach, that results in a procedure a bit different from those mentioned above. The advantage of this procedure is that we are able to derive non-linear semiclassical corrections within the functional integral formulation. The result is an infinite series of terms where higher non-linear terms are less important. We find that that the most important non-linear correction coincides with the one calculated in Ref. [4]. This correction is derived using the Keldysh formalism. However, due to the complication of the Keldysh indices and not to interrupt the flow of the section, we derive rigorously more terms using the Matsubara formalism in Appendix A.

Low-energy physics being restricted around the two Fermi points for free fermions is at the base of bosonization. The addition of weak local interactions between fermions smears the average occupation around the Fermi points, in addition to the smearing due to the temperature. However, the Fermi points, $\pm p_F$, are not modified by the presence of interactions as a consequence of the Luttinger's theorem [22, 23, 24]. The Hamiltonian of a system of interacting fermionic particles is,

$$\hat{H} = \int dx \hat{\psi}^\dagger(x) \left[-\frac{\partial_x^2}{2m} - \varepsilon_F \right] \hat{\psi}(x) + \frac{1}{2} \int dx dx' : \hat{\psi}^\dagger(x) \hat{\psi}(x) V(x-x') \hat{\psi}^\dagger(x') \hat{\psi}(x') :, \quad (11)$$

where $\hat{\psi}(x)$ is the fermionic field operator, m the mass of fermions, $V(x-x')$ a local density-density interaction and the colons denotes normal order of operators. In the functional integral representation, the partition function corresponding to Hamiltonian (11) is,

$$Z = \int \mathcal{D}[\bar{\psi}, \psi] e^{i \int_{\rightleftharpoons} dt \left[\int dx \bar{\psi}(x,t) \left(i\partial_t + \frac{\partial_x^2}{2m} + \varepsilon_F \right) \psi(x,t) - \frac{1}{2} \int dx dx' \bar{\psi}(x,t) \psi(x,t) V(x-x') \bar{\psi}(x',t) \psi(x',t) \right]}, \quad (12)$$

where ψ and $\bar{\psi}$ are the Grassmann fields corresponding to $\hat{\psi}$ and $\hat{\psi}^\dagger$, \rightleftharpoons denotes the closed

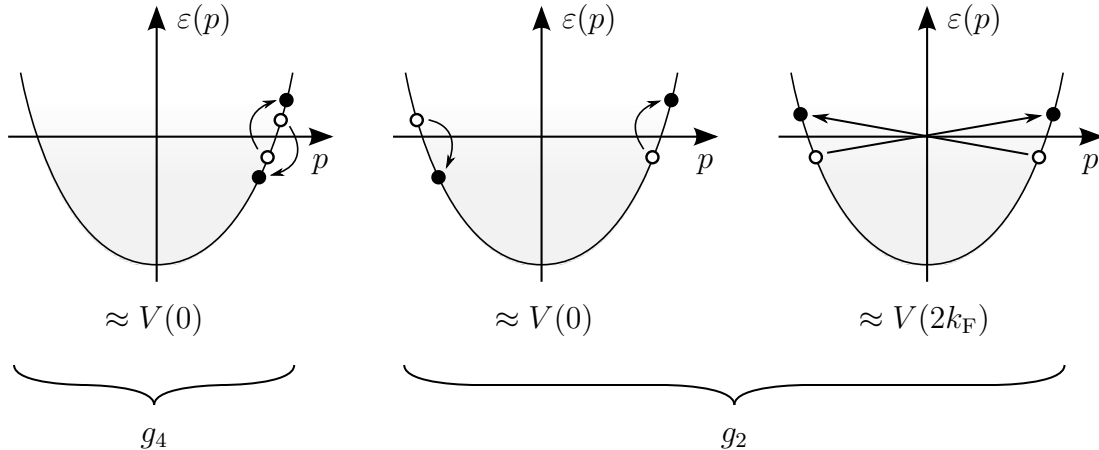


Figure 4: Relevant processes to the interaction term (14).

time contour⁴, and the thermal distribution in the infinite past has an average occupation,

$$n(p) = \frac{1}{e^{\beta(\varepsilon(p) - \varepsilon_F)} + 1}, \quad (13)$$

where $\varepsilon(p) = p^2/2m$ is the free fermionic spectrum. Now, we use the fact that, at low energies, the physics is constrained around the Fermi points in order to simplify the interaction term in partition function (12), that in momentum space reads,

$$-\frac{1}{2} \int dk dk' \frac{dq}{2\pi} V(q) \bar{\psi}(k - q, t) \psi(k, t) \bar{\psi}(k' + q, t) \psi(k', t). \quad (14)$$

Here, quantities in real space and momentum space are related by,

$$V(q) = \int dx V(x) e^{-iqx},$$

$$\psi(k, t) = \int dx \psi(x, t) e^{-ikx},$$

where we considered a system of infinite length. The density-density interaction term (14) is represented by two particle-hole excitations: two particles with momentum k and k' are annihilated and two with momentum $k - q$ and $k' + q$ are created. At small energies, this leads to the three processes depicted in Fig. 4. All the three processes have small total momentum and energy; however, while single particle-hole excitations in the first two processes have small momenta, $q \approx 0$, the ones in the third process have large momenta, $q \approx \pm 2k_F$, as particles move to opposite Fermi points. It is then convenient to split the fermion fields in the relevant parts, close to the Fermi points, and irrelevant ones, away

⁴ \rightleftharpoons corresponds to \mathcal{C} in Ref. [9].

from them,

$$\begin{aligned}
\psi(x, t) &= \int \frac{dk}{2\pi} \psi(k, t) e^{ikx} \\
&= e^{ik_F x} \int_{-q_0/2}^{q_0/2} \frac{dk}{2\pi} \psi(k_F + k, t) e^{ikx} + e^{-ik_F x} \int_{-q_0/2}^{q_0/2} \frac{dk}{2\pi} \psi(-k_F + k, t) e^{ikx} + \dots \quad (15) \\
&= e^{ik_F x} \psi_+(x, t) + e^{-ik_F x} \psi_-(x, t) + \dots,
\end{aligned}$$

where we introduced the momentum cut-off q_0 around the Fermi points to delimit the relevant from the irrelevant parts, represented by the dots. Since ψ_+ and ψ_- are only constituted by positive or negative momenta, they move respectively to the right and to the left; for this reason we call them right and left movers. Substituting decomposition (15) into partition function (12) we have,

$$\begin{aligned}
Z[u] &= \int \mathcal{D}[\bar{\psi}_\pm, \psi_\pm] e^{i \int_{\pm} dr \bar{\psi}_\eta(r) (G_\eta^{-1}(r) - u_\eta(r)) \psi_\eta(r)} \\
&\quad \times e^{-\frac{i}{2} \int_{\pm} dr \bar{\psi}_\eta(r) \psi_\eta(r) g_{\eta\eta'} \bar{\psi}_{\eta'}(r) \psi_{\eta'}(r)}, \quad (16)
\end{aligned}$$

where $\eta = \pm 1$, $r = (x, t)$, $dr = dxdt$ and we defined the bare Green's functions,

$$G_\eta^{-1}(r) = i\partial_t + \eta i v_F \partial_x + \frac{\partial_x^2}{2m}, \quad (17)$$

and the interaction matrix,

$$g_{\eta\eta'} = \begin{pmatrix} g_4 & g_2 \\ g_2 & g_4 \end{pmatrix},$$

$$g_4 \approx V(0),$$

$$g_2 \approx V(0) - V(2k_F).$$

We also integrated over the fields far away from the Fermi points, represented by the dots in decomposition (15), as they contribute only through the quadratic free propagator to the normalisation of the partition function. We added external source fields, $u_+(r)$ and $u_-(r)$, coupled to the densities of right and left movers, $\bar{\psi}_+(r)\psi_+(r)$ and $\bar{\psi}_-(r)\psi_-(r)$, to keep track of what these quantities become after bosonization. Now, we decouple the interaction term using a Hubbard-Stratonovich transformation,

$$Z[u] = \int \mathcal{D}\varrho_\pm e^{\frac{i}{2} \int_{\pm} dr \varrho_\eta g_{\eta\eta'}^{-1} \varrho_{\eta'}} Z_+[\varrho_+ + u_+] Z_-[\varrho_- + u_-],$$

where,

$$Z_\eta[\varrho] = \int \mathcal{D}[\bar{\psi}_\eta, \psi_\eta] e^{i \int_{\pm} dr \bar{\psi}_\eta (G_\eta^{-1} - \varrho) \psi_\eta},$$

is the non-interacting part of the partition function. Here and in the following we often omit the r dependence of the fields. We make the shift $\varrho \rightarrow \varrho - u$ and the partition function becomes,

$$Z[u] = \int \mathcal{D}\varrho_{\pm} e^{\frac{i}{2} \int_{\pm} dr (\varrho_{\eta} - u_{\eta}) g_{\eta\eta'}^{-1}(\varrho_{\eta'} - u_{\eta'})} Z_{+}[\varrho_{+}] Z_{-}[\varrho_{-}]. \quad (18)$$

The presence of the inverse interaction term is problematic when the interaction is zero, in the case of free fermions. To avoid this, in the spirit of Ref. [21], we make a second Hubbard-Stratonovich transformation,

$$Z[u] = \int \mathcal{D}\chi_{\pm} e^{i \int_{\pm} dr \left[-\frac{1}{2} \chi'_{\eta} \frac{1}{(2\pi)^2} g_{\eta\eta'} \chi'_{\eta'} - \frac{1}{2\pi} \chi'_{\eta} u_{\eta} \right]} \tilde{Z}_{+}[\chi_{+}] \tilde{Z}_{-}[\chi_{-}], \quad (19)$$

where χ_{\pm} are called right and left chiral fields, prime denotes a position derivative, $\chi' = \partial_x \chi$, and \tilde{Z}_{η} is the functional Fourier transform of Z_{η} ,

$$\tilde{Z}_{\eta}[\chi_{\eta}] = \int \mathcal{D}\varrho_{\eta} e^{i \int_{\pm} dr \frac{1}{2\pi} \chi'_{\eta} \varrho_{\eta}} Z_{\eta}[\varrho_{\eta}].$$

The reason for having ∂_x acting on χ is that, as we will see in the next subsection, the final result will be local in position space.⁵ After a Keldysh rotation, the partition function reads,

$$\begin{aligned} Z[u] &= \int \mathcal{D}\chi_{\pm} e^{i \int dr \left[-\frac{1}{2} \chi'^{\alpha}_{\eta} \left(\frac{1}{2\pi^2} g_{\eta\eta'} \right) \chi'_{\eta'}{}^{\alpha} - \frac{1}{\pi} \chi'^{\alpha}_{\eta} u_{\eta\alpha} \right]} \tilde{Z}_{+}[\chi_{+}] \tilde{Z}_{-}[\chi_{-}], \\ \tilde{Z}_{\eta}[\chi_{\eta}] &= \int \mathcal{D}\varrho_{\eta} e^{i \int dr \frac{1}{\pi} \chi'^{\alpha}_{\eta} \varrho_{\eta\alpha}} Z_{\eta}[\varrho_{\eta}], \\ Z_{\eta}[\varrho_{\eta}] &= \int \mathcal{D}[\bar{\psi}_{\eta}, \psi_{\eta}] e^{i \int_{-\infty}^{\infty} dr \bar{\psi}_{\eta}^{\alpha} \left[[G_{\eta}^{-1}]^{ab} - \varrho_{\eta}^{ab} \right] \psi_{\eta}^{\beta}}, \end{aligned} \quad (20)$$

where $[G_{\eta}^{-1}]^{ab}(x, t) = \delta^{ab} G_{\eta}^{-1}(x, t)$ is the inverse Green's function and $\varrho_{\eta}^{ab} = \delta^{ab} \varrho_{\eta}^{\text{cl}} + \sigma_1^{ab} \varrho_{\eta}^{\text{q}}$. For brevity, we omit the classical and quantum indices in the integration measure and we introduce the covariant-like notation $\varrho_{\alpha} = \sigma_1^{\alpha\beta} \varrho^{\beta}$, where $\sigma_1^{\alpha\beta}$ is the first Pauli matrix. We also omitted the infinitesimally small Keldysh component, $[G_{\eta}^{-1}]^{12}$ [9]. Here and in the following we include the normalisation factor of the partition function in the integration measure and use the fact that $Z = 1$ in absence of quantum sources. We evaluate $Z_{\eta}[\varrho_{\eta}]$

⁵The derivative also contributes to the normalisation of the partition function, that we include in the integration measure.

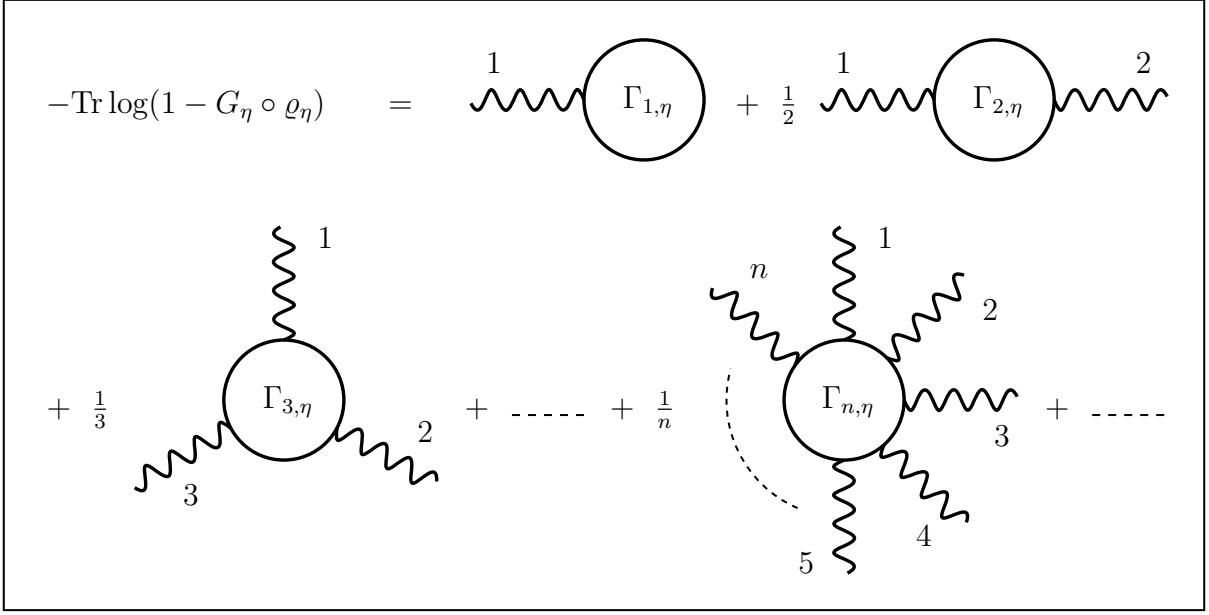


Figure 5: Diagrammatic representation of series (23). The wavy lines represent the fields ϱ_η 's and the solid lines the fermionic Green's functions, G_η 's. The fermionic loops $\Gamma_{n,\eta}$ are given by Eq. (24).

by integrating over right and left movers,

$$\begin{aligned}
Z_\eta[\varrho_\eta] &= \frac{\det(-iG_\eta^{-1} + i\varrho_\eta)}{\det(-iG_\eta^{-1})} \\
&= e^{\text{Tr} \log(-iG_\eta^{-1} + i\varrho_\eta) - \text{Tr} \log(-iG_\eta^{-1})} \\
&= e^{\text{Tr} \log(1 - G_\eta \circ \varrho_\eta)},
\end{aligned} \tag{21}$$

where the compact notation means,

$$\begin{aligned}
\varrho_\eta &= \varrho_\eta^{ab}(r) \delta^2(r - r'), \\
G_\eta^{-1} &= [G_\eta^{-1}]^{ab}(r) \delta^2(r - r'), \\
G_\eta &= G_\eta^{ab}(r - r').
\end{aligned}$$

Here G_η is the right or left movers Green's function and \circ denotes convolution with respect to position and time. Substituting result (21) into the second line of Eq. (20), we have,

$$\tilde{Z}_\eta[\chi_\eta] = \int \mathcal{D}\varrho_\eta e^{i \int dr \frac{1}{\pi} \chi_\eta^\alpha \varrho_{\eta\alpha} + \text{Tr} \log(1 - G_\eta \circ \varrho_\eta)}. \tag{22}$$

The trace of the logarithm can be expanded in the usual way [25], leading to the n-particle vertices for the field ϱ_η ,

$$\begin{aligned}
-\text{Tr} \log(1 - G_\eta \circ \varrho_\eta) &= \text{Tr}(G_\eta \circ \varrho_\eta) + \frac{1}{2} \text{Tr}(G_\eta \circ \varrho_\eta \circ G_\eta \circ \varrho_\eta) + \dots \\
&= \sum_{n \geq 1} \frac{1}{n} \int dr_1 \dots dr_n \Gamma_{n\eta}^{\alpha_1 \dots \alpha_n}(r_1, \dots, r_n) \varrho_\eta^{\alpha_1}(r_1) \dots \varrho_\eta^{\alpha_n}(r_n). \tag{23}
\end{aligned}$$

The interaction vertex is,

$$\Gamma_{n,\eta}^{\alpha_1 \dots \alpha_n}(r_1, \dots, r_n) = \sigma_{\alpha_1}^{a_1, a'_1} G_\eta^{a'_1 a_2}(r_1 - r_2) \sigma_{\alpha_2}^{a_2, a'_2} G_\eta^{a'_2 a_3}(r_2 - r_3) \dots \sigma_{\alpha_n}^{a_n, a'_n} G_\eta^{a'_n a_1}(r_n - r_1), \tag{24}$$

where $\sigma_\alpha^{a, a'} = \delta_{\alpha, \text{cl}} \delta^{aa'} + \delta_{\alpha, \text{q}} \sigma_1^{aa'}$. Series (23) is represented by means of the Feynman diagrams in Fig. 5. The wavy lines represent the fields ϱ_η 's and the solid lines the free fermion Green functions, G_η 's. The first term of the series, known as tadpole diagram, is $\sim \int dr \varrho_\eta^\alpha(r)$ and just contributes to the homogeneous density of the system [26]. We omit it by measuring the density from its constant homogeneous value. The second term of the series, known as polarisation diagram, contributes to the free propagator of ϱ_η and is the leading contribution in the bosonization procedure. The rest of the terms, $n \geq 3$, are the non-linear diagrams, generating interactions between the fields ϱ_η 's. Although the series of diagrams is infinite, in the limit of low energies non-linear corrections become smaller compared to the polarisation diagram, as we will see in the following. We proceed by considering the lowest approximation, that is, the polarisation diagram.

3.2 Linear spectrum

The lower the energy, the lower the momentum and the smaller the relevant region around the Fermi points. This means that we may choose a smaller cut-off, q_0 . The spectrum with the cut-off around the right Fermi point is represented in Fig. 6. The dashed line in the figure represents the linearised spectrum around the right Fermi point and it is clear that the smaller the cut-off, the smaller the contribution of the curvature. Then, in the limit $q_0 \ll mv_F$, in first approximation we may neglect the curvature. To do so, we consider the fermionic spectrum with momentum centred around the right or left Fermi points, $\pm p_F$,

$$\varepsilon(p) = \frac{p^2}{2m} - \varepsilon_F \longrightarrow \varepsilon_\eta(p) = \frac{(p - \eta p_F)^2}{2m} - \frac{p_F^2}{2m} = \eta v_{FP} p + \frac{p^2}{2m}.$$

The linear approximation amounts to neglecting the quadratic term, retaining only the linear one,

$$\varepsilon_\eta(p) \approx \eta v_{FP} p.$$

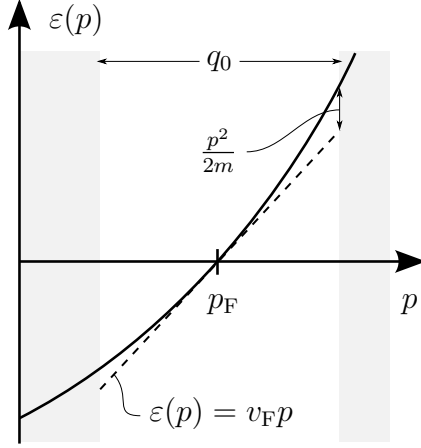


Figure 6: Linearisation of the spectrum, $\varepsilon(p) = v_F p + p^2/2m$, around the right Fermi point. The dashed line represents the linearised spectrum, $\varepsilon(p) = v_F p$, and q_0 is the cut-off introduced in the decomposition of the fermionic field into left and right movers, Eq. (15).

In the case of linear spectrum, Dzyaloshinski and Larkin proved that in equilibrium only the first two diagram in Fig. 5 are non-zero, that is, $\Gamma_{\eta,n} = 0$ for $n \geq 3$ in Eqs. (23) and (24) [27]. This statement goes by the name of the Dzyaloshinski-Larkin theorem. In the non-equilibrium case, an infinite series of non-linear terms in the quantum field is present, leading to an expansion in noise cumulants [20]. However, we neglect these terms by considering small deviations from equilibrium. Taking the linear spectrum approximation and using the Dzyaloshinski-Larkin theorem, Eq. (22) becomes,

$$\begin{aligned} \tilde{Z}_\eta[\chi_\eta] &= \int \mathcal{D}\varrho_\eta e^{i \int dr \frac{1}{\pi} \chi'_{\eta\alpha} \varrho_\eta^\alpha - \frac{i}{2} \int dr dr' \varrho_\eta^\alpha(r) \Pi_\eta^{\alpha\beta}(r-r') \varrho_\eta^\beta(r')} \\ &= \frac{1}{\sqrt{\det i\Pi_\eta}} e^{i \int dr dr' \frac{1}{2} \chi'_{\eta\alpha}(r) \frac{1}{\pi^2} [\Pi_\eta^{-1}]^{\alpha\beta}(r-r') \chi'_{\eta\beta}(r')}, \end{aligned}$$

where,

$$i\Pi_\eta^{\alpha\beta}(r) = \Gamma_{2,\eta}^{\alpha\beta}(r, -r) = \begin{pmatrix} 0 & i\Pi_\eta^A(r) \\ i\Pi_\eta^R(r) & i\Pi_\eta^K(r) \end{pmatrix}, \quad (25)$$

is the polarisation function of free fermions and,

$$\begin{aligned} i\Pi_\eta^R(x, t) &= [i\Pi_\eta^A(-x, -t)]^* \\ &= G_\eta^R(x, t) G_\eta^K(-x, -t) + G_\eta^K(x, t) G_\eta^A(-x, -t), \\ i\Pi_\eta^K(x, t) &= G_\eta^K(x, t) G_\eta^K(-x, -t) + G_\eta^R(x, t) G_\eta^A(-x, -t) + G_\eta^A(x, t) G_\eta^R(-x, -t) \\ &= G_\eta^K(x, t) G_\eta^K(-x, -t) - (G_\eta^R(x, t) - G_\eta^A(x, t)) (G_\eta^R(x, t) - G_\eta^A(x, t)), \end{aligned}$$

where in the last line we used,

$$\begin{aligned} G_\eta^{\text{R}}(x, t)G_\eta^{\text{R}}(-x, -t) &= 0, \\ G_\eta^{\text{A}}(x, t)G_\eta^{\text{A}}(-x, -t) &= 0, \end{aligned} \tag{26}$$

since their support is of null dimension [9]. The polarisation function is easier to calculate in the Fourier representation,

$$\varrho_\eta^\alpha(x, t) = \int \frac{dq}{2\pi} \frac{d\omega}{2\pi} \varrho_\eta^\alpha(q, \omega) e^{iqx - i\omega t},$$

that gives,

$$\tilde{Z}_\eta[\chi_\eta] = \frac{1}{\sqrt{\det i\Pi_\eta}} e^{i \int \frac{d\omega}{2\pi} \frac{dq}{2\pi} \frac{1}{2} \bar{\chi}_{\eta\alpha}(q, \omega) \frac{q^2}{\pi^2} [\Pi_\eta^{-1}]^{\alpha\beta}(q, \omega) \chi_{\eta\beta}(q, \omega)}, \tag{27}$$

where,

$$\begin{aligned} \Pi_\eta^{\text{R}}(q, \omega) &= [\Pi_\eta^{\text{A}}(q, \omega)]^* \\ &= -i \int \frac{dk}{2\pi} \frac{d\varepsilon}{2\pi} [G_\eta^{\text{R}}(k+q, \varepsilon+\omega)G_\eta^{\text{K}}(k, \varepsilon) + G_\eta^{\text{K}}(k+q, \varepsilon+\omega)G_\eta^{\text{A}}(k, \varepsilon)] \\ &= i \int \frac{dk}{2\pi} (F(\varepsilon_\eta(k)) - F(\varepsilon_\eta(k+q))) \int \frac{d\varepsilon}{2\pi} G_\eta^{\text{R}}(k+q, \varepsilon+\omega)G_\eta^{\text{A}}(k, \varepsilon), \\ \Pi_\eta^{\text{K}}(q, \omega) &= -i \int \frac{dk}{2\pi} \frac{d\varepsilon}{2\pi} [G_\eta^{\text{K}}(k+q, \varepsilon+\omega)G_\eta^{\text{K}}(k, \varepsilon) \\ &\quad - (G_\eta^{\text{R}}(k+q, \varepsilon+\omega) - G_\eta^{\text{A}}(k+q, \varepsilon+\omega)) (G_\eta^{\text{R}}(k, \varepsilon) - G_\eta^{\text{A}}(k, \varepsilon))] \\ &= -i \int \frac{dk}{2\pi} (F(\varepsilon_\eta(k+q))F(\varepsilon_\eta(k)) - 1) \\ &\quad \times \frac{d\varepsilon}{2\pi} (G_\eta^{\text{R}}(k+q, \varepsilon+\omega) - G_\eta^{\text{A}}(k+q, \varepsilon+\omega)) (G_\eta^{\text{R}}(k, \varepsilon) - G_\eta^{\text{A}}(k, \varepsilon)). \end{aligned}$$

Here we used the fluctuation-dissipation theorem to express the Keldysh component in terms of retarded and advanced ones,

$$\begin{aligned} G_\eta^{\text{K}}(k, \varepsilon) &= F(\varepsilon) (G_\eta^{\text{R}}(k, \varepsilon) - G_\eta^{\text{A}}(k, \varepsilon)) \\ &= F(\varepsilon_\eta(k)) (G_\eta^{\text{R}}(k, \varepsilon) - G_\eta^{\text{A}}(k, \varepsilon)). \end{aligned}$$

We also used the fact that Eqs. (26) imply,

$$\begin{aligned} \int \frac{d\varepsilon}{2\pi} G_\eta^{\text{R}}(k+q, \varepsilon+\omega)G_\eta^{\text{R}}(k, \varepsilon) &= 0, \\ \int \frac{d\varepsilon}{2\pi} G_\eta^{\text{A}}(k+q, \varepsilon+\omega)G_\eta^{\text{A}}(k, \varepsilon) &= 0. \end{aligned}$$

Using the thermal equilibrium average occupation, $F(\varepsilon) = \tanh\left(\frac{\varepsilon}{2T}\right)$, and integrating over ε , the retarded component of the polarisation function becomes,

$$\begin{aligned}\Pi_\eta^{\text{R}}(q, \omega) &= \frac{1}{\omega - \eta cq + i0} \int \frac{dk}{2\pi} \left[\tanh\left(\eta \frac{v_{\text{F}}k + v_{\text{F}}q}{2T}\right) - \tanh\left(\eta \frac{v_{\text{F}}k}{2T}\right) \right] \\ &= \frac{\eta}{\pi} \frac{q}{\omega - \eta cq + i0},\end{aligned}$$

and the Keldysh component,

$$\begin{aligned}\Pi_\eta^{\text{K}}(q, \omega) &= -i\delta(\omega - \eta v_{\text{F}}q) \int dk \left[1 - \tanh\left(\eta \frac{v_{\text{F}}k + v_{\text{F}}q}{2T}\right) \tanh\left(\eta \frac{v_{\text{F}}k}{2T}\right) \right] \\ &= -i\delta(\omega - \eta v_{\text{F}}q) \coth\left(\frac{cq}{2T}\right) \int dk \left[\tanh\left(\frac{v_{\text{F}}k + v_{\text{F}}q}{2T}\right) - \tanh\left(\frac{v_{\text{F}}k}{2T}\right) \right] \\ &= -2iq \coth\left(\frac{v_{\text{F}}q}{2T}\right) \delta(\omega - \eta v_{\text{F}}q),\end{aligned}$$

where in the second line we used the identity,

$$1 - \tanh(a) \tanh(b) = \coth(a - b) [\tanh(a) - \tanh(b)]. \quad (28)$$

Summarising, retarded, advanced and Keldysh Green's functions are,

$$\begin{aligned}\Pi_\eta^{\text{R,A}}(q, \omega) &= \frac{\eta}{\pi} \frac{q}{\omega - \eta v_{\text{F}}q \pm i0}, \\ \Pi_\eta^{\text{K}}(q, \omega) &= -2iq \coth\left(\frac{v_{\text{F}}q}{2T}\right) \delta(\omega - \eta v_{\text{F}}q), \\ &= \coth\left(\frac{\omega}{2T}\right) (\Pi_\eta^{\text{R}}(q, \omega) - \Pi_\eta^{\text{A}}(q, \omega)),\end{aligned}$$

where the last identity is a statement of the fluctuation-dissipation theorem. Now that we know the explicit form of the polarisation function, Eq. (25), we can invert it and substitute it in Eq. (27). The inverted polarisation Green's function reads,

$$[\Pi_\eta^{-1}(q, \omega)]^{\alpha\beta} = \Pi_\eta^{-1}(q, \omega) \sigma_1^{\alpha\beta} = \eta\pi \frac{\omega - \eta v_{\text{F}}q}{q} \sigma_1^{\alpha\beta},$$

where, as before, we omitted the infinitesimally small Keldysh component [9]. Substituting the inverse Green's function in Eq. (27) we have,

$$\tilde{Z}_\eta[\chi_\eta] = \frac{1}{\sqrt{\det i\Pi_\eta}} e^{i \int \frac{d\omega}{2\pi} \frac{dq}{2\pi} \frac{1}{2} \bar{\chi}_\eta^\alpha(q, \omega) D_{0, \eta}^{-1}(q, \omega) \chi_{\eta\alpha}(q, \omega)},$$

where we defined the propagator of the chiral fields without the contribution $\sim g_{\eta\eta'}$ from the density-density interactions of fermions (see first line of Eq. (20)) as,

$$D_{0,\eta}^{-1}(q, \omega) = \frac{q^2}{\pi^2} \Pi_\eta^{-1}(q, \omega) = \frac{\eta}{\pi} q(\omega - \eta v_F q).$$

Fourier transforming back to position and time, the partition function becomes,

$$Z_\eta[u] = \frac{1}{\sqrt{\det i\Pi_\eta}} e^{i \int dr \frac{1}{2} \chi_\eta^\alpha(r) D_{0,\eta}^{-1}(r) \chi_{\eta\alpha}(r)}, \quad (29)$$

where,

$$D_{0,\eta}^{-1}(r) = \frac{\eta}{\pi} \partial_x (\partial_t + \eta v_F \partial_x), \quad (30)$$

Finally, substituting Eqs. (29) into the first line in Eq. (20), we find the bosonized partition function of fermions with linear spectrum,

$$Z[u] = \int \mathcal{D}\chi_\pm e^{i \int dr \left[\frac{1}{2} \chi_\eta^\alpha D_{\eta\eta'}^{-1} \chi_{\eta'\alpha} - \frac{1}{\pi} \chi_\eta'^\alpha u_{\eta\alpha} \right]}, \quad (31)$$

where the chiral fields propagator is,

$$D_{\eta\eta'}^{-1}(r) = \delta_{\eta\eta'} D_{0,\eta}^{-1}(r) + \frac{1}{\pi} \frac{g_{\eta\eta'}}{2\pi} \partial_x^2. \quad (32)$$

The first thing that we note is that the exponent of partition function (31) is quadratic in χ_\pm . As hinted at the beginning of the section, this is a major advantage of bosonization: we started with a system of interacting electrons and we ended up with a quadratic low-energy theory that allows for exact analytical results. Thanks to the external source u_η we can relate the right and left chiral fields with right and left movers by comparing Eqs. (16) and (31), to obtain the correspondence,⁶

$$\bar{\psi}_\eta \psi_\eta \longleftrightarrow \frac{1}{2\pi} \partial_x \chi_\eta. \quad (33)$$

This means that $\frac{1}{2\pi} \partial_x \chi_\pm$ has the meaning of density of right and left movers. Partition function (31) is not the usual form found in literature [6]. The usual form corresponds to the expression in parenthesis of Eq. (3) and, to obtain it, we make the transformation,

$$\chi_\pm = \theta \pm \phi, \quad (34)$$

⁶Note that in this definition we dropped the Keldysh indices by writing the fields in the closed time contour, $\overleftrightarrow{}$, in order to meet the standard definitions found in literature [4, 5, 6, 7]. We also removed a factor 2 multiplying $\partial_x \chi_\eta^\alpha / 2\pi$ that appears Keldysh formalism (See also Ref. [9]). We will refer again to this footnote, for example for the fields θ and ϕ .

and find the Tomonaga-Luttinger liquid partition function,

$$Z[u] = \int \mathcal{D}\theta \mathcal{D}\phi e^{i \int dr} \left[\begin{pmatrix} \theta^\alpha \\ \phi^\alpha \end{pmatrix}^\top \begin{pmatrix} \frac{c}{\pi K} \partial_x^2 & \frac{1}{\pi} \partial_t \partial_x \\ \frac{1}{\pi} \partial_t \partial_x & \frac{cK}{\pi} \partial_x^2 \end{pmatrix} \begin{pmatrix} \theta_\alpha \\ \phi_\alpha \end{pmatrix} - \begin{pmatrix} \frac{2}{\pi} \partial_x \theta^\alpha \\ \frac{2}{\pi} \partial_x \phi^\alpha \end{pmatrix} \begin{pmatrix} u_{\theta\alpha} \\ u_{\phi\alpha} \end{pmatrix} \right] \quad (35)$$

where we defined,

$$c = \sqrt{\left(v_F + \frac{g_4}{2\pi}\right)^2 - \left(\frac{g_2}{2\pi}\right)^2}, \quad (36)$$

$$K = \sqrt{\frac{v_F + \frac{g_4}{2\pi} - \frac{g_2}{2\pi}}{v_F + \frac{g_4}{2\pi} + \frac{g_2}{2\pi}}},$$

Note that $c \approx v_F$ and $K \approx 1$ because the initial fermions are weakly interacting. We also defined the new source fields coupled to θ and ϕ in terms of the ones coupled to χ_\pm as,

$$u_{\theta,\phi} = \frac{u_+ \pm u_-}{2}$$

Relation (33) is now updated to,⁶

$$\begin{aligned} \bar{\psi}_+ \psi_+ + \bar{\psi}_- \psi_- &\longleftrightarrow \frac{1}{\pi} \partial_x \theta. \\ \bar{\psi}_+ \psi_+ - \bar{\psi}_- \psi_- &\longleftrightarrow \frac{1}{\pi} \partial_x \phi. \end{aligned} \quad (37)$$

The first line is the sum of the densities of right and left movers, which defines the non-homogeneous part of the density. Remembering that we are measuring the non-homogeneous part of the density from its homogeneous part, we find that $\frac{1}{\pi} \partial_x \theta$ measures the density fluctuations (in the low-energy limit). The term $\phi^\alpha \partial_t (\frac{1}{\pi} \partial_x \theta_\alpha)$ in partition function (35) is the term of the Legendre transform that relates the Lagrangian and the Hamiltonian, such as $p\dot{x}$ in $L = p\dot{x} - H$ in quantum mechanics. Then, in the same way p is conjugate to x , we deduce that ϕ is the phase conjugate to the density $\frac{1}{\pi} \partial_x \theta$. We conclude that we have obtained the hydrodynamic formalism given by the Luttinger liquid Hamiltonian, Eq. (3), without the non-linear corrections and the constant energy term.⁷ Therefore, the the parameter c and K in Eq. (36) are the speed of sound and the Luttinger parameter. From the second line of Eq. (37) and Eq. (2) we also find that the low-energy velocity field in terms of right and left movers is $v = \frac{\pi}{m} (\bar{\psi}_+ \psi_+ - \bar{\psi}_- \psi_-)$.

⁷For the comparison, note that there is an additional factor 2 multiplying the Lagrangian in the Keldysh formalism.

3.3 Non-linear corrections

In the last subsection we derived the linear bosonization, corresponding to the first two diagrams of Fig. 5. The first diagram was omitted by measuring the density from its homogeneous value and the second diagram led to a quadratic low-energy theory of hydrodynamic excitations. As part of the original contributions of this work, in this sub-section we derive the first non-linear correction to linear bosonization, the three-leg diagram in Fig. 5, within the Keldysh functional integral. We show that perturbation theory in the spectrum curvature works well to derive the three-leg correction. We check this result using a more rigorous approach based on the Matsubara formalism, derived in Appendix A, where we also derive the four-leg correction and formulate a conjecture for all other terms.

The non-linear part of series (23), given by the sum with $n \geq 3$, that we denote as $M_\eta[\varrho_\eta^\alpha]$, can be reformulated using the knowledge of the polarisation diagram. We split linear and non-linear parts of $\text{Tr} \log(1 - G_\eta \circ \varrho_\eta)$ in (22),

$$\tilde{Z}_\eta[\chi_\eta] = \int \mathcal{D}\varrho_\eta e^{i \int dr \frac{1}{\pi} \chi_\eta'^\alpha \varrho_{\eta\alpha} - \frac{i}{2} \int dr dr' \varrho_\eta^\alpha(r) \Pi_\eta^{\alpha\beta}(r-r') \varrho_\eta^\beta(r') - M_\eta[\varrho_\eta^\alpha]},$$

and express the non-linear term, $M_\eta[\varrho_\eta^\alpha]$, in terms of the functional Fourier transform field, $\chi_\eta'^\alpha$, by substituting ϱ_η^α with $-i\pi \frac{\delta}{\delta \chi_\eta'^\alpha}$ and moving $M_\eta[-i\pi \frac{\delta}{\delta \chi_\eta'^\alpha}]$ in front of the integral,

$$\begin{aligned} \tilde{Z}_\eta[\chi_\eta] &= e^{-M_\eta[-i\pi \frac{\delta}{\delta \chi_\eta'^\alpha}]} \int \mathcal{D}\varrho_\eta e^{i \int dr \frac{1}{\pi} \chi_\eta'^\alpha \varrho_{\eta\alpha} - \frac{i}{2} \int dr dr' \varrho_\eta^\alpha(r) \Pi_\eta^{\alpha\beta}(r-r') \varrho_\eta^\beta(r')} \\ &= e^{-M_\eta[-i\pi \frac{\delta}{\delta \chi_\eta'^\alpha}]} e^{i \int dr \frac{1}{2} \chi_\eta^\alpha D_{0,\eta}^{-1} \chi_{\eta\alpha}} \\ &= e^{i \int dr \frac{1}{2} \chi_\eta^\alpha D_{0,\eta}^{-1} \chi_{\eta\alpha}} \left[e^{-i \int dr \frac{1}{2} \chi_\eta^\alpha D_{0,\eta}^{-1} \chi_{\eta\alpha}} e^{-M_\eta[-i\pi \frac{\delta}{\delta \chi_\eta'^\alpha}]} e^{i \int dr \frac{1}{2} \chi_\eta^\alpha D_{0,\eta}^{-1} \chi_{\eta\alpha}} \right], \end{aligned}$$

where in the second line we integrated over ϱ_η and used the linear bosonization results (29) and (30) and in the third line we multiplied and divided by $e^{i \int dr \frac{1}{2} \chi_\eta^\alpha D_{0,\eta}^{-1} \chi_{\eta\alpha}}$. Expanding the first term in a Taylor series in $-i\pi \frac{\delta}{\delta \chi_\eta'^\alpha}$ and inserting $1 = e^{i \int dr \frac{1}{2} \chi_\eta^\alpha D_{0,\eta}^{-1} \chi_{\eta\alpha}} e^{-i \int dr \frac{1}{2} \chi_\eta^\alpha D_{0,\eta}^{-1} \chi_{\eta\alpha}}$ between each derivative, we obtain the shift $-i\pi \frac{\delta}{\delta \chi_\eta'^\alpha} \rightarrow -\eta \partial_\eta \chi_\eta^\alpha - i\pi \frac{\delta}{\delta \chi_\eta'^\alpha}$, where we defined,

$$\partial_\eta = \partial_t + \eta v_F \partial_x,$$

that leads to,

$$\tilde{Z}_\eta[\chi_\eta] = e^{i \int dr \frac{1}{2} \chi_\eta^\alpha D_{0,\eta}^{-1} \chi_{\eta\alpha} - M_\eta[-\eta \partial_\eta \chi_\eta^\alpha - i\pi \frac{\delta}{\delta \chi_\eta'^\alpha}]}.$$

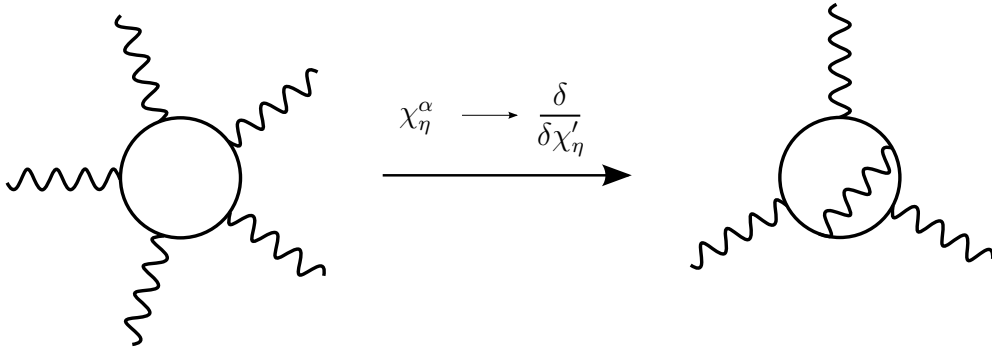


Figure 7: Example of contraction of two legs of the five-loop caused by the replacement of $\sim \chi_\eta^\alpha$ by $\sim \frac{\delta}{\delta\chi_\eta'}$ inside M_η in partition function (38). The contraction gives a correction to the semiclassical three-loop shown in Fig. 5.

Inserting this result in the first line of Eq. (20) and using Eq. (32) we find,

$$Z[u] = \int \mathcal{D}\chi_\pm e^{i \int dr \left[\frac{1}{2} \chi_\eta^\alpha D_{\eta\eta'}^{-1} \chi_{\eta'\alpha} - \frac{1}{\pi} \partial_x \chi_\eta^\alpha u_{\eta\alpha} \right] - \sum_\eta M_\eta \left[-\eta \partial_\eta \chi_\eta^\alpha - i\pi \frac{\delta}{\delta\chi_\eta^\alpha} \right]}. \quad (38)$$

This partition function contains two contributions in the exponent: the first term is the linear contribution found previously and the second term is the non-linear contribution. The argument of M_η is the sum of two terms, $\sim \chi_\eta^\alpha$ and $\sim \frac{\delta}{\delta\chi_\eta^\alpha}$. Let us explore what this means by considering the fifth power in the expansion of M_η from Eq. (23). If the derivative term, $\sim \frac{\delta}{\delta\chi_\eta^\alpha}$, were not present, we would have a term proportional to the product of five fields $\chi_\eta \chi_\eta \chi_\eta \chi_\eta \chi_\eta$, where we omitted variables and indices for brevity. The presence of $\sim \frac{\delta}{\delta\chi_\eta^\alpha}$ summed to $\sim \chi_\eta^\alpha$ in the power series, means that we consider terms where $\sim \chi_\eta^\alpha$ is replaced by $\sim \frac{\delta}{\delta\chi_\eta^\alpha}$, such as $\sim \chi_\eta \chi_\eta \chi_\eta \frac{\delta}{\delta\chi_\eta^\alpha} \chi_\eta \sim \chi_\eta \chi_\eta \chi_\eta$, where in the second step we acted with the derivative. Following this example, we see that replacing $\sim \chi_\eta^\alpha$ with $\sim \frac{\delta}{\delta\chi_\eta^\alpha}$ in the power series expansion of M_η amounts to reducing by two the number of fields in each term. By doing the explicit calculation it is easy to show that this generates contractions between pairs of fields χ_η^α , as shown in Fig. 7 in the case of five fields. Because contractions between pairs of fields generate quantum corrections [26], neglecting the derivative in the argument of M_η amounts to discarding quantum corrections, leading to a semiclassical approximation. Moreover, as we show in Appendix A, the quantum corrections are small for small momenta and, because we are considering the case $q \ll mc$, we can neglect them by dropping the term $\sim \frac{\delta}{\delta\chi_\eta^\alpha}$,

$$M_\eta \left[-\eta \partial_\eta \chi_\eta^\alpha - i\pi \frac{\delta}{\delta\chi_\eta^\alpha} \right] \stackrel{\text{semiclassical}}{\approx} M_\eta \left[-\eta \partial_\eta \chi_\eta^\alpha \right].$$

In the semiclassical approximation, we start exploring the first non-linear correction in

M_η , that is, the three-leg vertex, whose additional term to the action is,

$$S_{\text{nl}}[\chi_\eta^\alpha] = \frac{\eta}{3} \int dr_1 dr_2 dr_3 \Gamma_{3,\eta}^{\alpha_1 \alpha_2 \alpha_3}(r_1, r_2, r_3) \partial_\eta \chi_\eta^{\alpha_1}(r_1) \partial_\eta \chi_\eta^{\alpha_2}(r_2) \partial_\eta \chi_\eta^{\alpha_3}(r_3). \quad (39)$$

More specifically, since the main contribution in the semiclassical approximation is given by the equation of χ_η^{cl} [9], we need the product of two classical fields and one quantum field,

$$S_{\text{nl}}[\chi_\eta^\alpha] = \frac{\eta}{3} \int dr_1 dr_2 dr_3 \Gamma_{3,\eta}^{\text{clclq}}(r_1, r_2, r_3) \partial_\eta \chi_\eta^{\text{cl}}(r_1) \partial_\eta \chi_\eta^{\text{cl}}(r_2) \partial_\eta \chi_\eta^{\text{q}}(r_3), \quad (40)$$

where the vertex is,

$$\begin{aligned} \Gamma_{3,\eta}^{\text{clclq}}(r_1, r_2, r_3) &= G_\eta^{\text{R}}(r_1 - r_2) G_\eta^{\text{K}}(r_2 - r_3) G_\eta^{\text{R}}(r_3 - r_1) \\ &\quad + G_\eta^{\text{K}}(r_1 - r_2) G_\eta^{\text{A}}(r_2 - r_3) G_\eta^{\text{R}}(r_3 - r_1) \\ &\quad + G_\eta^{\text{A}}(r_1 - r_2) G_\eta^{\text{A}}(r_2 - r_3) G_\eta^{\text{K}}(r_3 - r_1). \end{aligned}$$

To calculate the vertex we Fourier transform,

$$\begin{aligned} -\frac{i\eta}{3} \int dQ_1 dQ_2 \Gamma_{3,\eta}^{\text{clclq}}(Q_1, Q_2) (\omega_1 - \eta c q_1) \chi_\eta^{\text{cl}}(Q_1) (\omega_2 - \eta c q_2) \chi_\eta^{\text{cl}}(Q_2) \\ \times (\omega_1 + \omega_2 - \eta c (q_1 + q_2)) \chi_\eta^{\text{q}}(-Q_1 - Q_2), \end{aligned}$$

where we use the shorthand notation $Q_i = (q_i, \omega_i)$ and,

$$\begin{aligned} \Gamma_{3,\eta}^{\text{clclq}}(Q_1, Q_2) &= \int \frac{dk}{2\pi} \frac{d\varepsilon}{2\pi} [G_\eta^{\text{R}}(K) G_\eta^{\text{K}}(K + Q_1) G_\eta^{\text{R}}(K + Q_1 + Q_2) \\ &\quad + G_\eta^{\text{K}}(K) G_\eta^{\text{A}}(K + Q_1) G_\eta^{\text{R}}(K + Q_1 + Q_2) \\ &\quad + G_\eta^{\text{A}}(K) G_\eta^{\text{A}}(K + Q_1) G_\eta^{\text{K}}(K + Q_1 + Q_2)]. \end{aligned}$$

Integrating over ε we have,

$$\begin{aligned} \Gamma_{3,\eta}^{\text{clclq}}(Q_1, Q_2) &= \\ &= -i \int \frac{dk}{2\pi} \left[-\frac{\tanh(\varepsilon_\eta(k + q_1)/2T)}{[\omega_1 - \varepsilon_\eta(k + q_1) + \varepsilon_\eta(k)][\omega_2 - \varepsilon_\eta(k + q_1 + q_2) + \varepsilon_\eta(k + q_1)]} \right. \\ &\quad + \frac{\tanh(\varepsilon_\eta(k)/2T)}{[\omega_1 - \varepsilon_\eta(k + q_1) + \varepsilon_\eta(k)][\omega_1 + \omega_2 - \varepsilon_\eta(k + q_1 + q_2) + \varepsilon_\eta(k)]} \\ &\quad \left. + \frac{\tanh(\varepsilon_\eta(k + q_1 + q_2)/2T)}{[\omega_2 - \varepsilon_\eta(k + q_1 + q_2) + \varepsilon_\eta(k + q_1)][\omega_1 + \omega_2 - \varepsilon_\eta(k + q_1 + q_2) + \varepsilon_\eta(k)]} \right], \end{aligned}$$

where $\varepsilon_\eta(k) = \eta c k + k^2/2m$. We split the first term using the identity $1/ab = (1/a +$

$1/b)/(a+b)$ and get

$$\begin{aligned} \Gamma_{3,\eta}^{\text{clclq}}(Q_1, Q_2) = & \\ = i \int \frac{dk}{2\pi} & \left[\frac{\tanh(\varepsilon_\eta(k+q_1)/2T) - \tanh(\varepsilon_\eta(k)/2T)}{[\omega_1 - \varepsilon_\eta(k+q_1) + \varepsilon_\eta(k)][\omega_1 + \omega_2 - \varepsilon_\eta(k+q_1+q_2) + \varepsilon_\eta(k)]} \right. \\ & \left. - \frac{\tanh(\varepsilon_\eta(k+q_1+q_2)/2T) - \tanh(\varepsilon_\eta(k+q_1)/2T)}{[\omega_2 - \varepsilon_\eta(k+q_1+q_2) + \varepsilon_\eta(k+q_1)][\omega_1 + \omega_2 - \varepsilon_\eta(k+q_1+q_2) + \varepsilon_\eta(k)]} \right]. \end{aligned}$$

We expand the integral up to the second power in the small spectrum curvature, m^{-1} , which, as we saw previously, is equivalent to a small momentum expansion, $q \ll k_F$. This expansion is convergent term by term and the first two are calculated more rigorously in Appendix A using the Matsubara formalism. As the vertices are symmetric for the exchange of external legs, we consider only their symmetrised part. The zero order symmetrised term in $1/m$ is zero, consistent with the Dzyaloshinski-Larkin theorem. Up to the third order we have,

$$\Gamma_{3,\eta}^{\text{clclq}}(Q_1, Q_2) = -\frac{i\eta}{2\pi m} \frac{q_1 q_2 (q_1 + q_2)}{(\omega_1 - \eta c q_1)(\omega_2 - \eta c q_2)(\omega_1 + \omega_2 - \eta c (q_1 + q_2))} + \mathcal{O}(m^{-3}).$$

This result is already symmetric and does not need symmetrisation. We also multiplied by a factor 3, as there are three ways of choosing the quantum field in Eq. (39). We note the absence of the second order term in m^{-1} . Then, Eq. (40) becomes,

$$iS_{\text{nl}}[\chi_\eta^\alpha] \approx \frac{1}{2\pi m} \int dQ_1 dQ_2 q_1 \chi_\eta^{\text{cl}}(Q_1) q_2 \chi_\eta^{\text{cl}}(Q_2) (q_1 + q_2) \chi_\eta^{\text{q}}(-Q_1 - Q_2).$$

Taking the Fourier transform we have,

$$S_{\text{nl}}[\chi_\eta^\alpha] = -\frac{1}{2\pi m} \int dr (\chi_\eta^{\text{cl}}(r))^2 \chi_\eta^{\text{q}}(r), \quad (41)$$

and adding this term to the quadratic part of the action in partition function (31), we have,

$$Z[u] = \int \mathcal{D}\chi_\pm \exp i \int dr \left[\frac{1}{2} \chi_\eta^\alpha D_{\eta\eta'}^{-1} \chi_{\eta'\alpha} - \frac{1}{2\pi m} (\chi_\eta^{\text{cl}})^2 \chi_\eta^{\text{q}} - \frac{1}{\pi} \chi_\eta^\alpha u_{\eta\alpha} \right].$$

Moreover, in the $\theta - \phi$ representation the non-linear term (41) becomes,

$$S_{\text{nl}}[\theta^\alpha, \phi^\alpha] = -\frac{1}{\pi m} \int dr \left\{ \left[(\theta^{\text{cl}}(r))^2 + (\phi^{\text{cl}}(r))^2 \right] \theta^{\text{q}}(r) + 2\theta^{\text{cl}}(r) \phi^{\text{cl}}(r) \phi^{\text{q}}(r) \right\}. \quad (42)$$

For the chiral fields, χ_\pm , and the phase fields, θ and ϕ , the mass curvature, m^{-1} , becomes the parameter that control the interaction.

The three-leg correction, being proportional to the mass curvature, is smaller and smaller the closer we are to the Fermi points or the smaller the cut-off, q_0 , is, as can be understood by Fig. 6. This fact, however, does not exclude the presence of higher non-linear terms, such as the four-leg diagram in Fig. 5. To exclude them, we have to show that higher non-linear terms are smaller than the three-leg term in the mass curvature. In support of this fact, at zero temperature, we have the Dzyaloshinski-Larkin theorem discussed previously. But, we can have a better feel by using dimensional analysis. By rescaling the n -leg contribution, Eq. (24), by the characteristic energy and momentum of the system, mv_F^2 and mv_F , we find that the n -loop behaves as $\tilde{\Gamma}_n \sim (mv_F^2)^{-(n-2)}$, where we defined $\tilde{\Gamma}_{n,\eta}$ as the symmetrised n -leg vertex for a correct treatment of n -loops, as seen in Appendix A.⁸ In turn, we have $\tilde{\Gamma}_{n+1}/\tilde{\Gamma}_n \sim m^{-1}$, that means that for a smaller spectrum curvature, m^{-1} , higher n -loop corrections become increasingly weaker. At finite but small temperatures, $T \ll mv_F^2$, the result must be consistent with the one at zero temperature in the limit of $T \rightarrow 0$, which implies that the thermal corrections to the n -loop can only have positive powers of the temperature, $\tilde{\Gamma}_n \sim T^\ell$, $\ell \geq 1$. Putting the zero and finite temperature dimensional analysis together, we conclude that the n -loop can only contain terms of the type,

$$\tilde{\Gamma}_n \sim (mv_F^2)^{-(n-2)} \left(\frac{T}{mv_F^2} \right)^\ell, \quad \ell \geq 0$$

and the term with $\ell = 0$ corresponds to the zero temperature contribution. So, in first approximation in $T/mv_F^2 \ll 1$, we have a small temperature extension of the Dzyaloshinski-Larkin theorem,

1. $\tilde{\Gamma}_n = \mathcal{O}(m^{-(n-2)})$ for $m^{-1} \rightarrow 0$;
2. $\tilde{\Gamma}_n$ does not depend on temperature at the lowest order in m^{-1} , that is, $m^{-(n-2)}$.

We verify this result in Appendix A for the three-, four- and five-loop and find $\tilde{\Gamma}_3 = \mathcal{O}(m^{-1})$, $\tilde{\Gamma}_4 = \mathcal{O}(m^{-2})$ and $\tilde{\Gamma}_5 = \mathcal{O}(m^{-3})$. Moreover, in the expansion in powers of m^{-1} , the first non-zero terms, respectively proportional to $\tilde{\Gamma}_3 \sim m^{-1}$, $\tilde{\Gamma}_4 \sim m^{-2}$ and $\tilde{\Gamma}_5 \sim m^{-3}$, are temperature independent.

Within this argument, successive terms of series (23), given by fermionic loops with an increasing number of phononic external legs as in Fig. 5, are smaller and smaller in the spectrum curvature or closer to the Fermi points, justifying the dropping of loops with more than three legs for small momenta.

⁸Note that the characteristic energy and momentum coming from the fermionic interaction terms, $\sim g_2$ and $\sim g_4$, do not participate in the evaluation of the n -loop corrections.

4 Boson hydrodynamics

In the previous section we derived a low-energy hydrodynamic description of weakly interacting fermionic particles in one dimension using the technique of functional bosonization. In this section, we derive the low-energy hydrodynamic description of bosonic particles with repulsive contact interaction in the limits of weak and strong interaction.

The Lagrangian of the system is,

$$L[\bar{\varphi}, \varphi] = \int dx \left[\bar{\varphi} \left(i\partial_t + \frac{1}{2m} \partial_x^2 + \mu \right) \varphi - \frac{g}{2} (\bar{\varphi}\varphi)^2 \right], \quad (43)$$

where $\varphi(x, t)$ is the bosonic particle field, m is the mass of the particle, μ the chemical potential and g the interaction strength of the density-density interaction. The system described by Lagrangian (43) is homogeneous as it is not subject to any external potential. Then, we consider the mean homogeneous density of the system, n , and distinguish two cases [28, 14]:

1. Weak interaction or high density, $mg \ll n$;
2. Strong interaction or low density, $mg \gg n$ (Tonks-Girardeau gas);⁹

We start from the simpler case of weak interaction.

4.1 Weak interactions

For weak interactions or high density, it is useful to introduce the healing length, $\xi = \frac{1}{2\sqrt{mgn}}$, the characteristic length of the interacting system. The number of particles within a healing length is $n\xi = \frac{1}{2}\sqrt{\frac{n}{mg}} \propto \sqrt{n}$ and increases with density. At high densities, there are many particles in a healing length, satisfying the criterion for the applicability of the mean field theory [14]. Then, the dominant contribution to the functional integral is the mean field solution $\varphi = \bar{\varphi} = \sqrt{n}$ and minimisation of the energy $H[\bar{\varphi}, \varphi] = \int dx \bar{\varphi} i\partial_t \varphi - L[\bar{\varphi}, \varphi]$ gives the condition,

$$\mu = gn. \quad (44)$$

Now, we consider small fluctuations of the bosonic field, φ , around its mean value, \sqrt{n} . To do this, we write the bosonic field using the phase-density representation,

$$\varphi(x, t) = \sqrt{n + \rho(x, t)} e^{i\phi(x, t)}, \quad (45)$$

⁹Reintroducing \hbar , the left and right terms in the inequalities read $\hbar n$ and mg/\hbar . Setting $\hbar = 1$, n and mg have the dimensions of a momentum.

where ρ and ϕ are small density and phase fluctuations. Substituting phase-density representation (45) in Lagrangian (43) we find,

$$L[\rho, \phi] = \int dx \left[-\rho \partial_t \phi - \frac{n}{2m} (\partial_x \phi)^2 - \frac{g}{2} \rho^2 - \frac{1}{2m} \rho (\partial_x \phi)^2 - \frac{1}{8m} \frac{(\partial_x \rho)^2}{n + \rho} \right], \quad (46)$$

where we omitted constant and boundary terms. The last term is called quantum pressure and accounts for quantum effects. As we consider small density fluctuations, ρ , that is, fluctuations with size greater than the healing length, the quantum pressure can be neglected [14]. Comparing this hydrodynamic Lagrangian with Hamiltonian (1), the compressibility of the system is $\kappa = 1/gn^2$ and, as one would expect, it is harder to compress the system when the repulsion is stronger or the density is higher. Expressing the density in term of the phase θ , as $\rho = \frac{1}{\pi} \partial_x \theta$, the Lagrangian becomes,

$$L[\theta, \phi] = \int dx \left[-\frac{1}{\pi} \partial_x \theta \partial_t \phi - \frac{n}{2m} (\partial_x \phi)^2 - \frac{g}{2\pi^2} (\partial_x \theta)^2 - \frac{1}{2m\pi} \partial_x \theta (\partial_x \phi)^2 \right],$$

where the first three terms are the linear part and the last term the non-linear part. Integrating by parts we have,

$$L[\theta, \phi] = \int dx \frac{1}{2} \begin{pmatrix} \theta \\ \phi \end{pmatrix}^T \begin{pmatrix} \frac{c}{\pi K} \partial_x^2 & \frac{1}{\pi} \partial_t \partial_x \\ \frac{1}{\pi} \partial_t \partial_x & \frac{cK}{\pi} \partial_x^2 \end{pmatrix} \begin{pmatrix} \theta \\ \phi \end{pmatrix} - \int dx \left[\frac{1}{2m\pi} \partial_x \theta (\partial_x \phi)^2 \right], \quad (47)$$

where,

$$\begin{aligned} c &= \sqrt{\frac{ng}{m}}, \\ \frac{K}{\pi} &= \sqrt{\frac{n}{mg}}, \end{aligned} \quad (48)$$

are the speed of sound and the Luttinger parameter. Finally, we consider the action $S[\theta, \phi] = \int_{\square} dt L[\theta, \phi]$ and perform a Keldysh rotation to find the hydrodynamic action: the linear part is the same as the fermionic one, Eq. (35); however, the non-linear part does not contain the term cubic in $\partial_x \theta$, present in the fermionic case, Eq. (42).

4.2 Strong interactions

In the case of strong interaction or low density, the system becomes a Tonks-Girardeau gas of hard-core bosons [29, 30]. The partition function can be written as

$$\begin{aligned} Z &= \int \mathcal{D}[\bar{\varphi}, \varphi] e^{i \int dt dx [\bar{\varphi}(i\partial_t + \frac{1}{2m}\partial_x^2 + \mu)\varphi - \frac{g}{2}\bar{\varphi}^2\varphi^2]} \\ &= \int \mathcal{D}[\bar{\varphi}, \varphi] e^{i \int dt dx [\bar{\varphi}(i\partial_t + \frac{1}{2m}\partial_x^2 + \mu)\varphi]} \int \mathcal{D}[\bar{\xi}, \xi] e^{i \int dt dx [\frac{2}{g}\bar{\xi}\xi + \xi\bar{\varphi}^2 + \bar{\xi}\varphi^2]}, \end{aligned}$$

where in the second line we introduced the field ξ through a Hubbard-Stratonovich transformation. The last term in the limit $g \gg n/m$ becomes,

$$\begin{aligned} \int \mathcal{D}[\bar{\xi}, \xi] e^{i \int dt dx [\frac{2}{g}\bar{\xi}\xi + \xi\bar{\varphi}\bar{\varphi} + \bar{\xi}\varphi\varphi]} &\approx \int \mathcal{D}[\bar{\xi}, \xi] e^{i \int dt dx [\xi\bar{\varphi}\bar{\varphi} + \bar{\xi}\varphi\varphi]} = \\ &= \delta(\text{Re}(\varphi^2))\delta(\text{Im}(\varphi^2)) \\ &= \delta(\bar{\varphi}^2)\delta(\varphi^2), \end{aligned}$$

which imposes the constraint $\varphi(x)\varphi(x) = \bar{\varphi}(x)\bar{\varphi}(x) = 0$, that is, two bosons cannot be at the same position.¹⁰ The partition function simplifies to

$$Z = \int \mathcal{D}[\bar{\varphi}, \varphi] \delta(\bar{\varphi}^2)\delta(\varphi^2) e^{i \int dt dx [\bar{\varphi}(i\partial_t + \frac{1}{2m}\partial_x^2 + \mu)\varphi]}. \quad (49)$$

The constraint means that the boson fields anti-commute at the same position, $[\varphi(x), \varphi(x)]_- = 2\varphi(x)\varphi(x) = 0$, and commute at different positions, $[\varphi(x), \varphi(x')]_+ = 0$, $x \neq x'$. The anti-commutation property suggests to change the bosonic complex fields $\varphi(x)$ and $\bar{\varphi}(x)$ to the fermionic Grassmann fields $\psi(x)$ and $\bar{\psi}(x)$. Through the anti-commutativity of the fermions, the constraint $\varphi(x)\varphi(x) = \psi(x)\psi(x) = 0$ is automatically satisfied. However, the change of variables must respect the commutativity $[\varphi(x), \varphi(x')] = 0$ for $x \neq x'$. In other words, moving a boson through other bosons must not produce any change of sign. However, moving a fermion through an odd number of fermions produces a minus sign. This minus sign can be compensated by a phase factor through a Jordan-Wigner transformation [25],

$$\varphi(x) = \psi(x) e^{i\pi \int_{-\infty}^x dy \bar{\psi}(y)\psi(y)} \quad (50)$$

¹⁰Note that, alternatively, the interaction term can be split as $\int \mathcal{D}\varrho e^{i \int dt dx [\frac{1}{2g}\varrho^2 + \varrho\bar{\varphi}\varphi]}$, which, in the limit $mg \gg n$, would lead to the constraint $\bar{\varphi}(x)\varphi(x) = 0$. However, this imposes that the density is zero or, in other words, that there are no particles in the system. Having no particles in the system implies that no two bosons are at the same position, but the constraint that two bosons cannot be at the same position does not imply that there are no particles in the system. Therefore, for a more general constraint we need the weaker condition, that is, two bosons cannot be at the same position.

The integral at the exponent, $\int_{-\infty}^x dy \bar{\psi}(y)\psi(y) = \int_{-\infty}^x dy \sum_{j \in \text{particles}} \delta(y - y_j)$, counts the number of particles at the left of position x . Therefore, the minus sign coming from moving a fermion through an odd number of fermions is compensated by the one coming from the phase factor. Substituting Eq. (50) into partition function (49) and using the Grassmann variable identities, $\psi^2 = \bar{\psi}^2 = 0$, we obtain

$$Z = \int \mathcal{D}[\bar{\psi}, \psi] e^{i \int dt dx [\bar{\psi}(i\partial_t + \frac{1}{2m}\partial_x^2 + \mu)\psi]}$$

This shows that a system of strongly-interacting or hard-core bosons can be mapped into a system of free fermions. As a consequence, the chemical potential corresponds to the ground state energy of a system of fermions with density n , that is, $\mu = (\pi n)^2/2m = \varepsilon_F$. It follows that the Tonks-Girardeau gas of hard-core bosons is mapped into the Tomonaga-Luttinger liquid with,

$$\begin{aligned} c &= v_F = \frac{\pi n}{m}, \\ K &= 1. \end{aligned} \tag{51}$$

5 Refermionization

So far, we have derived the low-energy hydrodynamic theory, Eq. (3), starting from interacting fermionic or bosonic particles. In the case of weakly interacting fermions, the speed of sound, c , and the Luttinger parameter, K , are given by Eqs. (36) and the coefficient characterising the cubic density non-linearity is $\alpha = \pi^2/m$. In the case of weakly interacting bosons, c and K are given by Eqs. (48) and $\alpha = 0$. Instead, we saw that strongly interacting bosons behave like free fermions, leading to c and K given by Eqs. (51) and $\alpha = \pi^2/m$. Corresponding to the quadratic part of hydrodynamic Hamiltonian (3) are action (35) for fermions and the quadratic part of action (47) for bosons. These actions are not diagonal and it would be interesting to know what the excitations of the systems are by diagonalising them. First, we rescale the phase fields θ and ϕ to the effective phase fields $\tilde{\theta}$ and $\tilde{\phi}$ as $\theta = \sqrt{K} \tilde{\theta}$ and $\phi = \tilde{\phi}/\sqrt{K}$ and the quadratic part of the action becomes,

$$S_0[\tilde{\theta}^\alpha, \tilde{\phi}^\alpha] = \int dr \left[\begin{pmatrix} \tilde{\theta}^\alpha \\ \tilde{\phi}^\alpha \end{pmatrix}^T \begin{pmatrix} \frac{c}{\pi} \partial_x^2 & \frac{1}{\pi} \partial_t \partial_x \\ \frac{1}{\pi} \partial_t \partial_x & \frac{c}{\pi} \partial_x^2 \end{pmatrix} \begin{pmatrix} \tilde{\theta}_\alpha \\ \tilde{\phi}_\alpha \end{pmatrix} - \begin{pmatrix} \frac{2\sqrt{K}}{\pi} \partial_x \tilde{\theta}^\alpha \\ \frac{2}{\pi\sqrt{K}} \partial_x \tilde{\phi}^\alpha \end{pmatrix} \begin{pmatrix} u_{\theta\alpha} \\ u_{\phi\alpha} \end{pmatrix} \right].$$

This action is equal in form to the hydrodynamic action of non-interacting fermions with a renormalised Fermi velocity c and a rescaled coupling to the source fields. Since the action of non-interacting fermions is diagonal in the chiral fields representation, the action

is diagonalised by a transformation to the effective chiral fields $\tilde{\chi}_{\pm} = \tilde{\theta} \pm \tilde{\phi}$,

$$S_0[\tilde{\chi}_{\eta}^{\alpha}] = \int dr \left[\frac{1}{2} \tilde{\chi}_{\eta}^{\alpha} \tilde{D}_{0,\eta}^{-1} \tilde{\chi}_{\eta\alpha} - \frac{2\sqrt{K}}{\pi} \partial_x (\tilde{\chi}_{+}^{\alpha} + \tilde{\chi}_{-}^{\alpha}) u_{\theta\alpha} - \frac{2}{\pi\sqrt{K}} \partial_x (\tilde{\chi}_{+}^{\alpha} - \tilde{\chi}_{-}^{\alpha}) u_{\phi\alpha} \right],$$

where,

$$\tilde{D}_{0,\eta}^{-1}(r) = \frac{\eta}{\pi} \partial_x (\partial_t + \eta c \partial_x), \quad (52)$$

is the inverse propagator (30) with a renormalised sound velocity, c . Now we turn to the non-linear part of the action.

The non-linear terms are different for fermions and bosons. We start with fermions. In terms of the rescaled fields $\tilde{\theta}$ and $\tilde{\phi}$, the non-linear part of the fermionic hydrodynamic action, Eq. (42), becomes,

$$S_{\text{nl}}[\tilde{\theta}^{\alpha}, \tilde{\phi}^{\alpha}] = -\frac{1}{\pi m} \int dr \left\{ \left[K(\tilde{\theta}'^{\text{cl}})^2 + \frac{1}{K}(\tilde{\phi}'^{\text{cl}})^2 \right] \sqrt{K} \tilde{\theta}'^{\text{q}} + \frac{2}{\sqrt{K}} \tilde{\theta}'^{\text{cl}} \tilde{\phi}'^{\text{cl}} \tilde{\phi}'^{\text{q}} \right\},$$

and in terms of the effective chiral fields, $\tilde{\chi}_{\pm}$, we have,

$$\begin{aligned} S_{\text{nl}}[\tilde{\chi}_{\eta}^{\alpha}] &= -\frac{1}{2\pi m^*} \int dr (\tilde{\chi}_{\eta}^{\text{cl}})^2 \tilde{\chi}_{\eta}^{\text{q}} \\ &+ \frac{1}{8\pi m} \frac{1}{\sqrt{K}} (1 - K^2) \int dr [(\tilde{\chi}_{\bar{\eta}}^{\text{cl}})^2 + 2\tilde{\chi}_{\bar{\eta}}^{\text{cl}} \tilde{\chi}_{\eta}^{\text{cl}}] \tilde{\chi}_{\eta}^{\text{q}}, \end{aligned} \quad (53)$$

where $\bar{\eta}$ is the opposite of η and we defined the effective mass,

$$m^* = m \frac{4\sqrt{K}}{3 + K^2} \approx m \left(1 - \frac{3}{8} \delta K^2 \right) \quad (54)$$

where we expanded the Luttinger parameter in the weak interaction limit, $K = 1 + \delta K$ with $\delta K \ll 1$.

In the case of weakly interacting bosons, the non-linear part in Eq. (47) does not have the density-cube term, $\sim \theta'^3$, present in the fermionic one, Eq. (42). Rescaling the fields, Eq. (47) becomes,

$$S_{\text{nl}}[\tilde{\theta}^{\alpha}, \tilde{\phi}^{\alpha}] = -\frac{1}{\pi\sqrt{K}m} \int dr \left\{ (\tilde{\phi}'^{\text{cl}})^2 \tilde{\theta}'^{\text{q}} + 2\tilde{\theta}'^{\text{cl}} \tilde{\phi}'^{\text{cl}} \tilde{\phi}'^{\text{q}} \right\},$$

and in terms of $\tilde{\chi}_{\pm}$ we have,

$$\begin{aligned} S_{\text{nl}}[\tilde{\chi}_{\eta}^{\alpha}] &= -\frac{1}{2\pi m^*} \int dr (\tilde{\chi}_{\eta}^{\text{cl}})^2 \tilde{\chi}_{\eta}^{\text{q}} \\ &+ \frac{1}{8\pi m} \frac{1}{\sqrt{K}} \int dr [(\tilde{\chi}_{\bar{\eta}}^{\text{cl}})^2 + 2\tilde{\chi}_{\bar{\eta}}^{\text{cl}} \tilde{\chi}_{\eta}^{\text{cl}}] \tilde{\chi}_{\eta}^{\text{q}} \end{aligned} \quad (55)$$

where we defined the effective mass,

$$m^* = \frac{4}{3}m\sqrt{K}, \quad (56)$$

and we remind that for weakly interacting bosons $K \gg 1$.

In the non-linear actions (53) and (55) the first line describes interactions between effective chiral fields moving in the same directions, either $\eta = +1$ or $\eta = -1$; instead, the second line describes mixed interactions between right, $\eta = +1$, and left, $\eta = -1$, effective chiral fields. Since the interaction time between chiral fields moving in opposite directions is negligible compared to that of those moving in the same direction, we neglect the second lines of Eqs. (53) and (55). Then, the hydrodynamic partition functions for fermionic and bosonic particles have the same form,

$$Z[u] = \int \mathcal{D}\tilde{\chi}_\pm e^{i\int dr \left[\frac{1}{2}\tilde{\chi}_\eta^\alpha \tilde{D}_{0,\eta}^{-1} \tilde{\chi}_{\eta\alpha} - \frac{1}{2\pi m^*} (\tilde{\chi}_\eta^{\text{cl}})^2 \tilde{\chi}_\eta^{\text{cl}} - \frac{2\sqrt{K}}{\pi} \partial_x (\tilde{\chi}_+^\alpha + \tilde{\chi}_-^\alpha) u_{\theta\alpha} - \frac{2}{\pi\sqrt{K}} \partial_x (\tilde{\chi}_+^\alpha - \tilde{\chi}_-^\alpha) u_{\phi\alpha} \right]}. \quad (57)$$

Integrating over the quantum component of right and left chiral field [9], we obtain the equations of motion for the classical component,

$$(\partial_t + \eta c \partial_x) \tilde{\chi}_\eta^{\text{cl}} = -\frac{\eta}{2m^*} (\tilde{\chi}_\eta^{\text{cl}})^2, \quad (58)$$

where we omitted the source fields.

Partition function (57) looks like the partition function of bosonized free fermions with effective mass m^* and a different coupling to density and phase source fields u_θ and u_ϕ . Comparing the transformation between fermionic fields and chiral fields, Eq. (33), we transform to the effective fermionic fields $\tilde{\psi}$ and $\tilde{\bar{\psi}}$ as,⁶

$$\frac{1}{2\pi} \partial_x \tilde{\chi}_\eta \longleftrightarrow \tilde{\bar{\psi}}_\eta \tilde{\psi}_\eta.$$

Then, the effective chiral fields partition function, Eq. (57), corresponds to the effective fermions partition function,

$$Z[u] = \int \mathcal{D}[\tilde{\bar{\psi}}_\pm, \tilde{\psi}_\pm] e^{i\int dr \left[\tilde{\bar{\psi}}_\eta(r) \tilde{G}_\eta^{-1}(r) \tilde{\psi}_\eta(r) - \sqrt{K} (\tilde{\bar{\psi}}_+ \tilde{\psi}_+ + \tilde{\bar{\psi}}_- \tilde{\psi}_-) u_{\theta\alpha} - \frac{1}{\sqrt{K}} (\tilde{\bar{\psi}}_+ \tilde{\psi}_+ - \tilde{\bar{\psi}}_- \tilde{\psi}_-) u_{\phi\alpha} \right]}, \quad (59)$$

where the Green's functions is,

$$\tilde{G}_\eta^{-1}(r) = i\partial_t + \eta ic \partial_x + \frac{\partial_x^2}{2m^*}, \quad (60)$$

which leads to the spectrum,

$$\varepsilon_\eta(k) = \eta ck + \frac{k^2}{2m^*}. \quad (61)$$

The coupling to the source fields tells us that density and phase in terms of the effective fermions are $\sqrt{K}(\bar{\psi}_+\tilde{\psi}_+ + \bar{\psi}_-\tilde{\psi}_-)$ and $(\bar{\psi}_+\tilde{\psi}_+ - \bar{\psi}_-\tilde{\psi}_-)/\sqrt{K}$. These relations together with Eqs. (59) and (60) are known as refermionization. We do not prove it rigorously here and we refer to Refs. [31, 32, 33] for a rigorous derivation.

As in the case of bosonization, for which the non-linearity of the spectrum must be small, $k \ll mv_F$, for refermionization to be possible the condition $k \ll m^*c$ must hold. An additional condition in the case of weakly interacting bosons requires $p \ll p_G$, where $p_G = 4(m/m^*)mc = 3mc/\sqrt{K}$ is the Ginzburg momentum [34, 35]. The reason is that, only for momenta smaller than p_G the spectrum of weakly interacting bosons is quadratic [34, 35, 36], which is one of requirement for refermionization. The Ginzburg momentum is found by comparing the value of the momentum for which the quadratic spectrum,

$$\varepsilon(p) = cp + \frac{p^2}{2m^*}, \quad p \ll p_G,$$

crosses over to the Bogoliubov spectrum,

$$\varepsilon(p) = cp\sqrt{1 + \frac{p^2}{4m^2c^2}} \approx cp + \frac{p^3}{8m^2c}, \quad p \gg p_G.$$

The two energies match at momentum p_G , where we used Eq. (56) for the value of the effective mass. As $K \gg 1$ for weakly interacting bosons, the condition for the validity of refermionization is restrictive because $p_G \ll mc$. Finally, we note that fermionic quasiparticles are lighter than the initial particles, $m^* < m$, for interacting fermions and heavier, $m^* > m$, for weakly interacting bosons.

6 Particle-excitation map

In this work we derived the low-energy hydrodynamic and the fermionic quasiparticle theories for interacting fermionic and bosonic particles. The relations between these theories are depicted in Fig. 8 with the help of Feynman diagrams. We started from fermions, the top-right box in Fig. 8. The fermionic theory is characterised by the propagator and the local density-density interaction term, represented by the straight line and the cross diagrams. The propagator depends on the Fermi velocity, v_F , and mass, m , and the interaction terms correspond to scattering with strengths g_2 and g_4 between two fermions. Using functional bosonization, we showed that the low-energy particle-hole excitations around the two Fermi points give rise to phononic excitations. The theory of

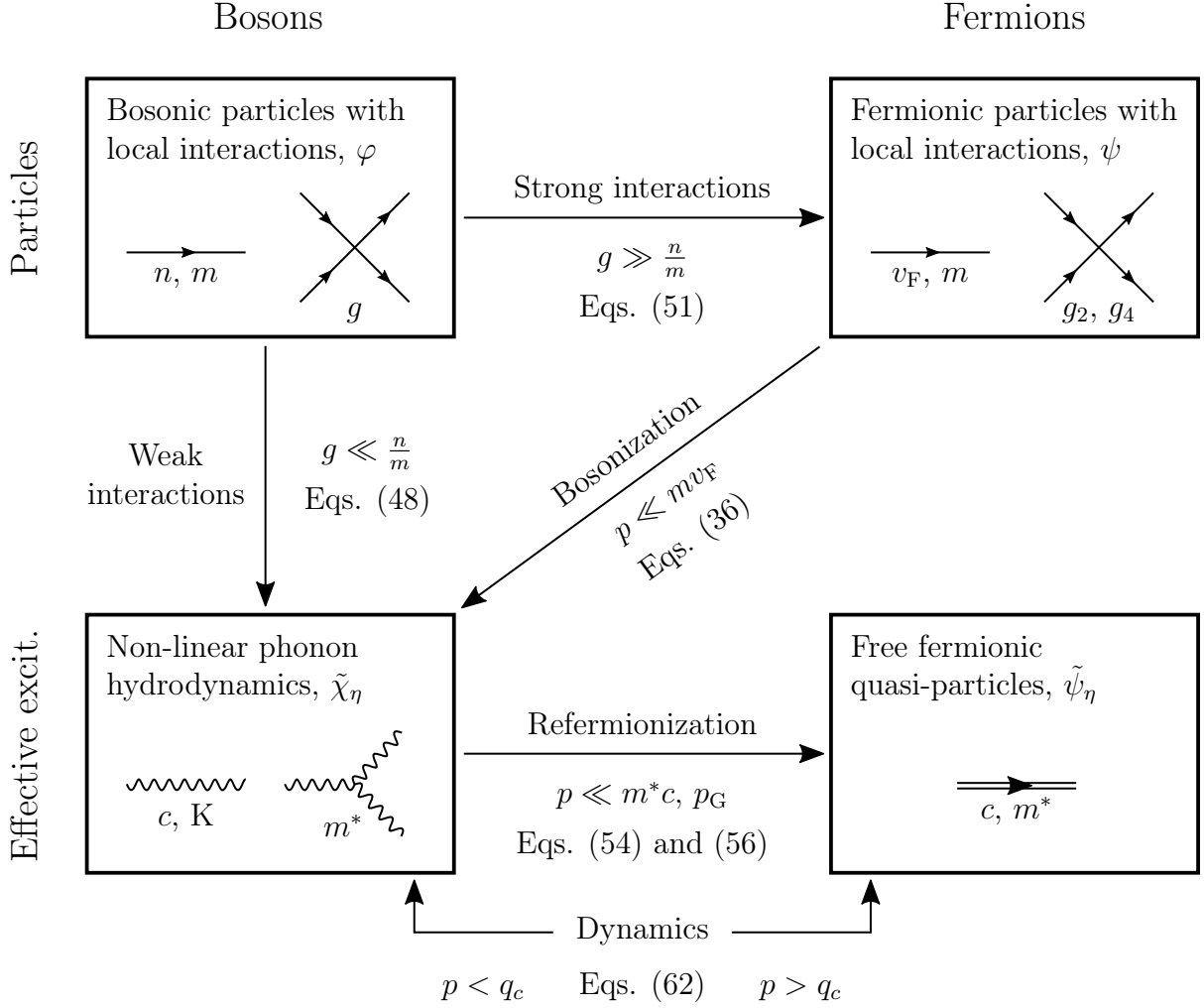


Figure 8: Schematic summary of the main results of this work. Left and right columns refer to bosonic and fermionic statistics and top and bottom rows to particles and effective excitations. The equation references give the relation between the parameters of the related theories.

phononic excitations is characterised by the two diagrams in the bottom-left box in Fig. 8. The wiggly line is the phonon propagator that depends on the speed of sound, c , and the Luttinger parameter, K . The three-leg diagram represents the non-linear contribution proportional to m^* that comes from the mass curvature, m , of the fermionic spectrum and corresponds to the three-loop of Fig. 5. This non-linear term, as suggested by the diagram, corresponds to the processes of splitting a phonon into two or recombining two into one. Additional non-linear terms with more legs are present, but can be neglected for small momenta, $p \ll mv_F$. Then, we considered bosonic particles with contact interactions, the top-left box in Fig. 8. The bosonic theory is characterised by the propagator and the contact density-density interaction term, represented by the straight line and the cross diagrams. The propagator depends on the density, n , and mass, m , and the interaction term corresponds to the scattering with strength g between two bosons. We considered

the two limits of weak and strong interactions. In the case of weak interactions, $g \ll \frac{n}{m}$, the hydrodynamic theory was derived in terms of density and phase fluctuations over the average values. In the case of strong interactions, $g \gg \frac{n}{m}$, bosons become impenetrable, a feature that allows the mapping to free fermions and, in turn, to the hydrodynamic theory with $K = 1$. Finally, we mapped the non-linear hydrodynamic theory to free fermionic quasiparticles with an effective Fermi velocity c and an effective mass m^* , the bottom-right box in Fig. 8. The mapping requires the additional low-momentum condition $p \ll m^*c$ and in the case of weakly interacting bosons the additional condition $p \ll p_G \sim 1/\sqrt{K}$.

7 Dynamics at finite temperatures

Non-linear phonons and free fermionic quasiparticles are equally good at describing static properties [7]. However, this is not the case for dynamical ones. In fact, to realise this, it is sufficient to compare the dynamical structure factor, $S(q, \omega)$, calculated using the two representations. We have already calculated $S(q, \omega)$ using free fermions and the result is represented in Fig. 3. In the case of fermionic quasiparticles, Fermi velocity, v_F , and mass, m , are replaced by c and m^* but the width depends on q in the same way: $\delta\omega(q) \sim q^2$ at $T = 0$ and $\delta\omega_T(q) \sim q$ at $T > 0$. Using phonons, we start deriving the dynamical structure factor using the quadratic approximation. We do not need to do the calculation explicitly, we just need to know that the dynamical structure factor is non-zero where the spectrum of particle-holes excitations is non-zero. Because the quadratic phonons approximation corresponds to fermions with linearised spectrum, there is no spectrum curvature and particle-hole excitations can only satisfy the relation $\omega = cq$. It follows that the dynamical structure factor is a straight line with slope c and no width in the $q - \omega$ plane of Fig. 3. This result is in clear contrast with the one derived using fermionic quasiparticles. But we know that, when there are no interactions between fermions, particles and quasiparticles coincide, giving the correct result. Then, we may add the three-leg term to the quadratic phonons. With this term, the calculation of the width of the dynamical structure factor is not straightforward as it involves a self-consistent approach to avoid a resonant behaviour. We do not give the explicit calculation here and refer to Refs. [37, 38]. The resulting width is $\delta\omega(q) \sim q^2$ at $T = 0$ and $\delta\omega_T(q) \sim q^{3/2}$ at $T > 0$. Now, fermionic quasiparticles and phonons give the same result at $T = 0$ but differ at $T > 0$: even with the three-leg correction, the two representations lead to different thermal dynamics in the small-momentum limit, where the three-leg approximation should hold better. This leads to an apparent paradox: which one is the best representation to describe the thermal dynamics of one-dimensional systems, non-linear phonons or free fermionic quasiparticles? This question is answered in Refs. [8, 39] through the study of

the dynamical structure factor, which shows that, at momenta lower than

$$q_c = \frac{\pi^5}{128} [\Gamma'_0]^2 \frac{T^7}{m^* c^7}, \quad (62)$$

the dynamics is dominated by interacting phonons and, at momenta higher than q_c , the dynamics is dominated by free fermionic quasiparticles. Here, Γ'_0 is a parameter that depends on the specific details of the systems.

8 Conclusions

In this work we gave a self-contained presentation of non-linear bosonization and re-fermionization of one-dimensional quantum systems within the Keldysh functional integral. We started with the derivation of the Tomonaga-Luttinger liquid for a system of interacting fermions by considering the linear spectrum approximation, that amounts to neglecting the spectrum curvature. This is a good approximation at low energies, where there are mainly low-energy particle-hole excitations around the two Fermi points and works well for static systems. In order to study dynamical systems, where higher energies become important, we derived an infinite series of non-linear corrections arising from the fermionic spectrum curvature and calculated the first one, corresponding to the interaction between three phonons. The result, obtained within the Keldysh formalism, was checked against a more rigorous approach based on the Matsubara formalism, presented in the Appendix, by evaluating the low-energy asymptotic contribution of the three- and four-phonon interactions to the action and some properties of the five-phonon interaction. These results and dimensional analysis invited a conjecture on the asymptotic curvature and temperature dependence of the interaction terms between an arbitrary number of phonons.

To complement the bosonization of interacting fermions, we bosonized interacting bosonic particles in the weak and strong interaction limits. In the weak-interaction limit, the standard mean-field approach was sufficient to derive the effective phononic action, but the strong-interaction limit required a more creative solution by decoupling the interaction term with a Hubbard-Stratonovich transformation and showing how a system of bosons with infinite repulsive interaction can be restated as a system of free fermions.

Finally, we used the relation between non-linear phonons and interacting fermions to re-fermionize the system, that is, to derive an approximate theory of fermionic quasiparticles. This work culminates in a map between fermionic and bosonic particles and bosonic and fermionic excitations, that is, phonons and fermionic quasiparticles. In particular, we noticed that the description of one-dimensional quantum systems in term of phonons and fermionic quasiparticles should be equivalent. However, the dynamical structure factor

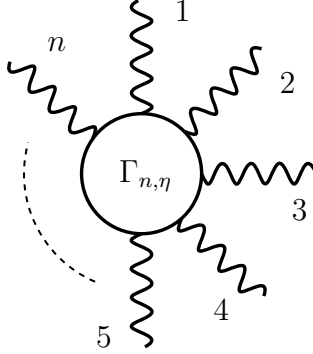


Figure 9: n-loop.

shows that, within the approximations that we considered, the equivalence applies only to static and zero-temperature dynamical properties and leads to different results for the thermal dynamics, where phonons and fermionic quasiparticles are better at describing respectively lower and higher momenta.

9 Acknowledgements

I am grateful to D. M. Gangardt, A. J. Kingl and M. Jones for helpful discussions. I acknowledge the support of the University of Birmingham.

A n-loop reduction formula

In this section we derive a reduction formula for the symmetrised fermionic n-loop by adapting the zero temperature derivation of Refs. [40, 41] to finite temperatures, T , using the Matsubara formalism. The fermionic n-loop is shown in Fig. 9 and is defined as (compare it with the analogous expression (24) in the Keldysh formalism),

$$\Gamma_n(Q_1, \dots, Q_{n-1}) = I_n(P_1, \dots, P_n) = -\frac{1}{\beta} \sum_{E_\ell} \int \frac{dk}{2\pi} G(K + P_1) \dots G(K + P_n),$$

where $Q_j = (\omega_j, q_j)$ are phononic momentum and Matsubara energy variables and $P_j = (\epsilon_j, p_j) = Q_1 + \dots + Q_j$ and $K = (E_\ell, k)$ are fermionic ones. The Matsubara Green's function is defined as,

$$G(K) = \frac{1}{iE_\ell - \varepsilon(k)},$$

and $\varepsilon(k) = v_{\text{F}}k + k^2/2m$ is the right mover spectrum. Here we limit the study to right movers as the results for left movers are symmetric. The sum over fermionic energies $E_\ell = \pi i(2\ell + 1)T$ is easily evaluated by means of the residue theorem and yields,

$$I_n(P_1, \dots, P_n) = \int \frac{dk}{2\pi} \sum_{i=1}^n n_i \prod_{\substack{j=1 \\ j \neq i}}^n \frac{1}{f_{ji}(k)},$$

where,

$$n_i = n_{\text{F}}(-i\epsilon_i + \varepsilon(k + p_i)),$$

is the occupation factor of a state with momentum p_i and energy ϵ_i and,

$$\begin{aligned} f_{ij}(k) &= (i\epsilon_i - \varepsilon(k + p_i)) - (i\epsilon_j - \varepsilon(k + p_j)) \\ &= (i\epsilon_i - \varepsilon(p_i)) - (i\epsilon_j - \varepsilon(p_j)) - \frac{p_i - p_j}{m}k. \end{aligned}$$

The n-loop can be rewritten as,

$$I_n(P_1, \dots, P_n) = \int \frac{dk}{2\pi} \sum_{i=1}^n n_i \prod_{\substack{j=1 \\ j \neq i}}^n \left(\frac{m}{p_{ij}} \right) \prod_{\substack{j=1 \\ j \neq i}}^n \left(\frac{1}{k - \Delta_{ij}} \right), \quad (63)$$

where $p_{ij} = p_i - p_j$ and,

$$\Delta_{ij} = \frac{m}{p_{ij}} [(i\epsilon_i - \varepsilon(p_i)) - (i\epsilon_j - \varepsilon(p_j))].$$

The last product in the n-loop (63) can be expressed as a sum using a partial fraction expansion,

$$\prod_{\substack{j=1 \\ j \neq i}}^n \left(\frac{1}{k - \Delta_{ij}} \right) = \sum_{\substack{j=1 \\ j \neq i}}^n \left[\frac{1}{k - \Delta_{ij}} \prod_{\substack{n=1 \\ n \neq i, j}}^n \left(\frac{1}{\Delta_{ij} - \Delta_{in}} \right) \right].$$

Then, the n-loop (63) becomes,

$$I_n(P_1, \dots, P_n) = \sum_{\substack{i, j=1 \\ i \neq j}}^n \left(\frac{m}{p_{ij}} \int \frac{dk}{2\pi} \frac{n_i}{k - \Delta_{ij}} \right) \prod_{\substack{n=1 \\ n \neq i, j}}^n \left(\frac{1}{f_{ij}^n} \right),$$

where,

$$\begin{aligned} f_{ij}^n &= \frac{p_{in}}{m} (\Delta_{ij} - \Delta_{in}) = i \frac{p_{jn}\epsilon_{in} - p_{in}\epsilon_{jn}}{p_{ij}} + \frac{p_{in}p_{jn}}{2m} \\ &= \frac{1}{p_{ij}} \left[p_{jl} \left(\tilde{\varepsilon}_i - \frac{p_i^2}{2m} \right) - p_{il} \left(\tilde{\varepsilon}_j - \frac{p_j^2}{2m} \right) + p_{ij} \left(\tilde{\varepsilon}_l - \frac{p_l^2}{2m} \right) \right]. \end{aligned}$$

Using the symmetries $f_{ij}^n = f_{ji}^n$ and $\Delta_{ij} = \Delta_{ji}$, we expressed the sum using the difference of occupation factors,

$$I_n(P_1, \dots, P_n) = \sum_{\substack{i,j=1 \\ i>j}}^n \left(\frac{m}{p_{ij}} \int \frac{dk}{2\pi} \frac{n_i - n_j}{k - \Delta_{ij}} \right) \prod_{\substack{n=1 \\ n \neq i,j}}^n \left(\frac{1}{f_{ij}^n} \right).$$

The term in the first parenthesis coincides with the two-loop,

$$\begin{aligned} I_2(P_i, P_j) &= -\frac{1}{\beta} \sum_{E_\ell} \int \frac{dk}{2\pi} G(K + P_i) G(K + P_j) \\ &= \frac{m}{p_{ij}} \int \frac{dk}{2\pi} \frac{n_i - n_j}{k - \Delta_{ij}}, \end{aligned} \tag{64}$$

shown in Fig. 10. Making the shift $K \rightarrow K - P_j$, we obtain,

$$I_2(P_i, P_j) = -\frac{1}{\beta} \sum_{E_\ell} \int \frac{dk}{2\pi} G(K + P_i - P_j) G(K) = I_2(P_i - P_j, 0) \equiv I_2(P_i - P_j).$$

The two-loop depends only on the differences $p_{ij} = p_i - p_j$ and $\epsilon_{ij} = \epsilon_i - \epsilon_j$ as a consequence of energy and momentum conservations. Finally, the reduction formula becomes,

$$I_n(P_1, \dots, P_n) = \sum_{\substack{i,j=1 \\ i>j}}^n I_2(P_{ij}) \prod_{\substack{n=1 \\ n \neq i,j}}^n \left(\frac{1}{f_{ij}^n} \right). \tag{65}$$

A.1 Two-loop

We rewrite the two-loop (64) as,

$$I_2(P_i, P_j) = -\frac{m}{4\pi p_{ij}} \int_{-\infty}^{\infty} dk \frac{\tanh\left(\frac{\epsilon(k+p_i)}{2T}\right) - \tanh\left(\frac{\epsilon(k+p_j)}{2T}\right)}{k - \Delta_{ij}},$$

In this form, a shift of the variable k cannot be taken separately for the two hyperbolic tangents, as only their difference is convergent at $k \rightarrow \pm\infty$. To allow for the shift to be taken for the two terms separately, we integrate by parts,

$$I_2(P_i, P_j) = \frac{m}{8\pi T p_{ij}} \int dk \log(k - \Delta_{ij}) \left[\frac{v_F + (k + p_i)/m}{\cosh^2\left(\frac{\epsilon(k+p_i)}{2T}\right)} - \frac{v_F + (k + p_j)/m}{\cosh^2\left(\frac{\epsilon(k+p_j)}{2T}\right)} \right].$$

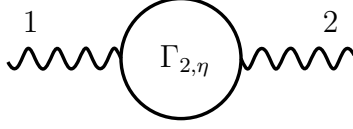


Figure 10: Two-loop.

Now the two terms converge separately and we make the shifts $k \rightarrow k - p_i$ in the first one and $k \rightarrow k - p_j$ in the second one to obtain,

$$\begin{aligned}
I_2(P_{ij}) &= \frac{m}{8\pi T p_{ij}} \int dk \log \left(\frac{k - p_i - \Delta_{ij}}{k - p_j - \Delta_{ij}} \right) \frac{v_F + k/m}{\cosh^2 \left(\frac{\varepsilon(k)}{2T} \right)} \\
&= \frac{m}{8\pi T p_{ij}} \int dk \log \left[\frac{\tilde{\epsilon}_{ij} - \frac{p_{ij}}{m} \left(k - \frac{p_{ij}}{2} \right)}{\tilde{\epsilon}_{ij} - \frac{p_{ij}}{m} \left(k + \frac{p_{ij}}{2} \right)} \right] \frac{v_F + k/m}{\cosh^2 \left(\frac{v_F k + k^2/2m}{2T} \right)},
\end{aligned} \tag{66}$$

where we defined $\tilde{\epsilon}_{ij} = i\epsilon_{ij} - v_F p_{ij}$, where the double index from now on denotes the difference, for example $\tilde{\epsilon}_{ij} = \tilde{\epsilon}_i - \tilde{\epsilon}_j$. At zero temperature,

$$\lim_{T \rightarrow 0} \frac{1}{4T \cosh^2 \left(\frac{v_F k + k^2/2m}{2T} \right)} = \delta \left(v_F k + \frac{k^2}{2m} \right).$$

The zeros of the argument of the delta function are at $k = 0$ and $k = -2mv_F = -2k_F$, but we can neglect the second zero as it describes a sub-leading contribution with momenta close to the the left Fermi point. Integrating over k , the two-loop simplifies to,

$$I_{2,0}(P_{ij}) = \frac{m}{2\pi p_{ij}} \log \left[\frac{\tilde{\epsilon}_{ij} + \frac{p_{ij}^2}{2m}}{\tilde{\epsilon}_{ij} - \frac{p_{ij}^2}{2m}} \right].$$

Noting that I_2 is even in m , an expansion in powers of m^{-1} at zero temperature reads,

$$I_{2,0}(P_{ij}) = \frac{m}{\pi p_{ij}} \sum_{\substack{n=1 \\ n \text{ odd}}}^{\infty} \frac{1}{n} \left(\frac{p_{ij}^2}{2m\tilde{\epsilon}_{ij}} \right)^n = \frac{1}{2\pi} \frac{p_{ij}}{\tilde{\epsilon}_{ij}} + \frac{1}{24\pi m^2} \frac{p_{ij}^5}{\tilde{\epsilon}_{ij}^3} + \mathcal{O}(m^{-4})$$

The dynamical condition for the convergence of the series is $p_{ij}^2 \ll m\tilde{\epsilon}_{ij}$. Instead, in the static limit, $\epsilon_i \rightarrow 0$, we have $\tilde{\epsilon}_{ij} \rightarrow -cp_{ij}$ and the condition for convergence becomes $|p_{ij}| = |q_i + \dots + q_{j-1}| \ll mv_F = k_F$, which means that the phononic momenta must be small compared to the Fermi momentum, as seen in Chap. 2. At finite temperatures, the two-loop gets an additional term dependent on T in the second term of the expansion in m^{-1} ,

$$I_2(P_{ij}) = \frac{1}{2\pi} \frac{p_{ij}}{\tilde{\epsilon}_{ij}} + \frac{1}{24\pi m^2} \frac{p_{ij}^2}{\tilde{\epsilon}_{ij}^3} \left[p_{ij}^3 + 2\pi^2 \frac{T^2}{c^3} (2cp_{ij} - \tilde{\epsilon}_{ij}) \right] + \mathcal{O}(m^{-4}).$$

Note that we did not expand in T .

A.2 Three-loop and four-loop

The three-loop, the first in Fig. 11, is given in terms of q_i and ω_i , by,

$$\begin{aligned}\Gamma_3(Q_1, Q_2) &= I_3(P_1 = 0, P_2 = Q_1, P_3 = Q_1 + Q_2) \\ &= \frac{q_1 I_2(Q_1) + q_2 I_2(Q_2) - (q_1 + q_2) I_2(Q_1 + Q_2)}{i(q_1 \epsilon_2 - q_2 \epsilon_1) + q_1 q_2 (q_1 + q_2) / 2m}.\end{aligned}$$

n-loops are symmetric by exchange of external legs. Therefore, we symmetrise by taking the circular permutations of Q_1 , Q_2 and Q_3 , which amount to summing $\Gamma_3(Q_1, Q_2)$ and $\Gamma_3(Q_2, Q_1)$. The symmetric part of the three loop is,

$$\begin{aligned}\tilde{\Gamma}_3(Q_1, Q_2) &= \Gamma_3(Q_1, Q_2) + \Gamma_3(Q_2, Q_1) \\ &= -\frac{q_1 q_2 (q_1 + q_2)}{2m} \frac{q_1 I_2(Q_1) + q_2 I_2(Q_2) - (q_1 + q_2) I_2(Q_1 + Q_2)}{(q_1 \epsilon_2 - q_2 \epsilon_1)^2 + (q_1 q_2 (q_1 + q_2) / 2m)^2}.\end{aligned}$$

An $m^{-1} \rightarrow 0$ power expansion reads,

$$\begin{aligned}\tilde{\Gamma}_3(Q_1, Q_2) &= \frac{1}{4\pi m} \frac{q_1 q_2 q_3}{\tilde{\omega}_1 \tilde{\omega}_2 \tilde{\omega}_3} \\ &+ \frac{1}{8\pi m^3} q_1 q_2 q_3 \left\{ \frac{1}{(q_2 \tilde{\omega}_1 - q_1 \tilde{\omega}_2)^2} \left[\frac{1}{2} \frac{q_1^2 q_2^2 q_3^2}{\tilde{\omega}_1 \tilde{\omega}_2 \tilde{\omega}_3} - \frac{1}{3} \left(\frac{q_1^6}{\tilde{\omega}_1^3} + \frac{q_2^6}{\tilde{\omega}_2^3} + \frac{q_3^6}{\tilde{\omega}_3^3} \right) \right. \right. \\ &\left. \left. - \frac{4}{3} \pi^2 \frac{T^2}{c^2} \left(\frac{q_1^4}{\tilde{\omega}_1^3} + \frac{q_2^4}{\tilde{\omega}_2^3} + \frac{q_3^4}{\tilde{\omega}_3^3} \right) \right] - \frac{2}{3} \pi^2 \frac{T^2}{c^3} \frac{q_1 \tilde{\omega}_2 \tilde{\omega}_3 + \tilde{\omega}_1 q_2 \tilde{\omega}_3 + \tilde{\omega}_1 \tilde{\omega}_2 q_3}{\tilde{\omega}_1^2 \tilde{\omega}_2^2 \tilde{\omega}_3^2} \right\} \\ &+ \mathcal{O}(m^{-5}),\end{aligned}$$

where $\tilde{\omega}_i = i\omega_i - v_F q_i$ and $Q_3 = -Q_1 - Q_2$. We note that at the first order in m^{-1} , the three-loop does not depend on temperature. Moreover, there is no term independent of m , which leads to $\lim_{m^{-1} \rightarrow 0} \tilde{\Gamma}_3 = 0$, consistent with the Dzyaloshinski-Larkin theorem (see page 16). Similarly, the symmetrised four-loop, the second in Fig. 11, is,

$$\tilde{\Gamma}_4(Q_1, Q_2, Q_3) = \frac{1}{4\pi m^2} \frac{q_1 q_2 q_3 q_4}{\tilde{\omega}_1 \tilde{\omega}_2 \tilde{\omega}_3 \tilde{\omega}_4} \left[\frac{q_1 + q_2}{\tilde{\omega}_1 + \tilde{\omega}_2} + \frac{q_1 + q_3}{\tilde{\omega}_1 + \tilde{\omega}_3} + \frac{q_2 + q_3}{\tilde{\omega}_2 + \tilde{\omega}_3} \right] + \mathcal{O}(m^{-4}).$$

As for the three-loop, at the first order in m^{-1} , the three-loop does not depend on temperature and it is consistent with the Dzyaloshinski-Larkin theorem, $\lim_{m^{-1} \rightarrow 0} \tilde{\Gamma}_4 = 0$. However, $\tilde{\Gamma}_4 = \mathcal{O}(m^{-2})$ goes to zero faster than $\tilde{\Gamma}_3 = \mathcal{O}(m^{-1})$ for $m^{-1} \rightarrow 0$. Moreover, it can be checked that the five-loop, the third in Fig. 11, is $\tilde{\Gamma}_5 = \mathcal{O}(m^{-3})$ for $m^{-1} \rightarrow 0$ and

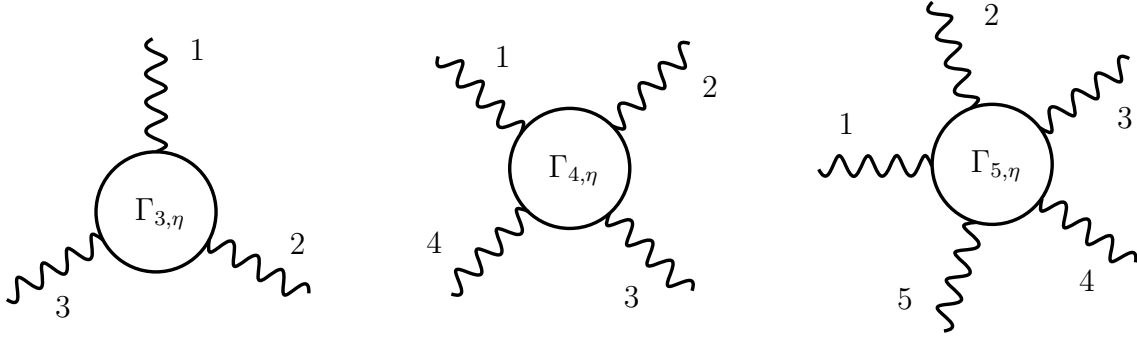


Figure 11: Three-loop, four-loop and five-loop.

at the lowest order, m^{-3} , $\tilde{\Gamma}_5$ does not depend on temperature.¹¹

References

- [1] S.-I. Tomonaga. Remarks on Bloch’s Method of Sound Waves applied to Many-Fermion Problems. *Progress of Theoretical Physics*, 5(4):544–569, 1950.
- [2] J. M. Luttinger. An Exactly Soluble Model of a Many-Fermion System. *Journal of Mathematical Physics*, 4(9):1154–1162, 1963.
- [3] D. C. Mattis and E. H. Lieb. Exact Solution of a Many-Fermion System and Its Associated Boson Field. *Journal of Mathematical Physics*, 6(2):304–312, 1965.
- [4] F. D. M. Haldane. ’Luttinger liquid theory’ of one-dimensional quantum fluids. I. Properties of the Luttinger model and their extension to the general 1D interacting spinless Fermi gas. *Journal of Physics C: Solid State Physics*, 14(19):2585, 1981.
- [5] F. D. M. Haldane. Effective Harmonic-Fluid Approach to Low-Energy Properties of One-Dimensional Quantum Fluids. *Phys. Rev. Lett.*, 47:1840–1843, 1981.
- [6] T. Giamarchi. *Quantum Physics in One Dimension*. International Series of Monographs on Physics. Oxford University Press, USA, 2004.
- [7] A. Imambekov, T. L. Schmidt, and L. I. Glazman. One-dimensional quantum liquids: Beyond the Luttinger liquid paradigm. *Rev. Mod. Phys.*, 84:1253–1306, 2012.
- [8] M. Arzamasovs, F. Bovo, and D. M. Gangardt. Kinetics of Mobile Impurities and Correlation Functions in One-Dimensional Superfluids at Finite Temperature. *Physical Review Letters*, 112(17):170602, 2014.

¹¹The symmetrisation was done numerically and was computationally too expensive for loops with more than five legs.

- [9] A. Kamenev. *Field Theory of Non-Equilibrium Systems*. Cambridge University Press, 2011.
- [10] V. N. Popov. *Functional Integrals and Collective Excitations*. Cambridge Monographs on Mathematical Physics. Cambridge University Press, 1991.
- [11] P. Nozieres and D. Pines. *Theory Of Quantum Liquids*. Advanced Books Classics Series. Westview Press, 1999.
- [12] J. Stenger, S. Inouye, A. P. Chikkatur, D. M. Stamper-Kurn, D. E. Pritchard, and W. Ketterle. Bragg Spectroscopy of a Bose-Einstein Condensate. *Phys. Rev. Lett.*, 82:4569–4573, 1999.
- [13] N. Fabbri, D. Clément, L. Fallani, C. Fort, and M. Inguscio. Momentum-resolved study of an array of one-dimensional strongly phase-fluctuating Bose gases. *Phys. Rev. A*, 83:031604, 2011.
- [14] L. Pitaevskii and S. Stringari. *Bose-Einstein Condensation*. International Series of Monographs on Physics. Oxford University Press, USA, 2003.
- [15] H. C. Fogedby. Correlation functions for the Tomonaga model. *Journal of Physics C: Solid State Physics*, 9(20):3757, 1976.
- [16] D. K. K. Lee and Y. Chen. Functional bosonisation of the Tomonaga-Luttinger model. *Journal of Physics A: Mathematical and General*, 21(22):4155, 1988.
- [17] I. V. Yurkevich. Bosonisation as the Hubbard Stratonovich Transformation. In I.V. Lerner, B.L. Althsuler, and V.I. Fal’ko, editors, *Strongly Correlated Fermions and Bosons in Low-Dimensional Disordered Systems*, NATO science series: Mathematics, physics, and chemistry. Springer, 2002.
- [18] A. Grishin, I. V. Yurkevich, and I. V. Lerner. Functional integral bosonization for an impurity in a Luttinger liquid. *Phys. Rev. B*, 69:165108, 2004.
- [19] I. V. Lerner and I. V. Yurkevich. Seminar 1 Impurity in the tomonaga-luttinger model: A functional integral approach. In H. Bouchiat, Y. Gefen, S. Guéron, G. Montambaux, and J. Dalibard, editors, *Nanophysics: Coherence and Transport École d’été de Physique des Houches Session LXXXI*, volume 81 of *Les Houches*, pages 109 – 127. Elsevier, 2005.
- [20] D. B. Gutman, Y. Gefen, and A. D. Mirlin. Bosonization of one-dimensional fermions out of equilibrium. *Phys. Rev. B*, 81:085436, 2010.

- [21] P. Kopietz. *Bosonization of Interacting Fermions in Arbitrary Dimensions*. Bosonization of Interacting Fermions in Arbitrary Dimensions. Springer Berlin Heidelberg, 1997.
- [22] J. M. Luttinger and J. C. Ward. Ground-State Energy of a Many-Fermion System. II. *Phys. Rev.*, 118:1417–1427, 1960.
- [23] J. M. Luttinger. Fermi Surface and Some Simple Equilibrium Properties of a System of Interacting Fermions. *Phys. Rev.*, 119:1153–1163, 1960.
- [24] A. M. Tsvelik. *Quantum Field Theory in Condensed Matter Physics*. Cambridge University Press, 2003.
- [25] A. Altland and B.D. Simons. *Condensed Matter Field Theory*. Cambridge University Press, 2010.
- [26] J. Zinn-Justin. *Quantum Field Theory and Critical Phenomena*. International series of monographs on physics. Clarendon Press, 2002.
- [27] I. E. Dzyaloshinskii and A. I. Larkin. Correlation functions for a one-dimensional Fermi system with long-range interaction (Tomonaga model). *Sov. Phys. JETP*, 38:202, 1974.
- [28] F. Dalfovo, S. Giorgini, L. P. Pitaevskii, and S. Stringari. Theory of Bose-Einstein condensation in trapped gases. *Rev. Mod. Phys.*, 71:463–512, 1999.
- [29] M. Girardeau. Relationship between Systems of Impenetrable Bosons and Fermions in One Dimension. *J. Math. Phys.*, 1(6):516, 1960.
- [30] E. H. Lieb and W. Liniger. Exact Analysis of an Interacting Bose Gas. I. The General Solution and the Ground State. *Phys. Rev.*, 130(4):1605, 1963.
- [31] A. V. Rozhkov. Fermionic quasiparticle representation of Tomonaga-Luttinger Hamiltonian. *Eur. Phys. J. B*, 47(2):193–206, 2005.
- [32] A. V. Rozhkov. Density-density propagator for one-dimensional interacting spinless fermions with nonlinear dispersion and calculation of the Coulomb drag resistivity. *Phys. Rev. B*, 77(12):1–5, 2008.
- [33] J. von Delft and H. Schoeller. Bosonization for beginners — refermionization for experts. *Annalen der Physik*, 7(4):225–305, 1998.
- [34] M. Pustilnik and K. A. Matveev. Low-energy excitations of a one-dimensional Bose gas with weak contact repulsion. *Phys. Rev. B*, 89:100504, 2014.

- [35] Z. Ristivojevic. Excitation Spectrum of the Lieb-Liniger Model. *Phys. Rev. Lett.*, 113:015301, 2014.
- [36] P. P. Kulish, S. V. Manakov, and L. D. Faddeev. Comparison of the exact quantum and quasiclassical results for a nonlinear Schrödinger equation. *Theor. Math. Phys.*, 28(1):615–620, 1976.
- [37] A. F. Andreev. The hydrodynamics of two- and one-dimensional liquids. *Sov. Phys. JETP*, 51:1038–1042, 1980.
- [38] K. V. Samokhin. Lifetime of excitations in a clean Luttinger liquid. *J. Phys. Cond. Mat.*, 10:533–538, 1998.
- [39] F. Bovo. Thermal dynamics of one-dimensional quantum systems. *PhD Thesis*, 2015.
- [40] A. Neumayr and W. Metzner. Fermion loops, loop cancellation, and density correlations in two-dimensional Fermi systems. *Phys. Rev. B*, 58:15449–15459, 1998.
- [41] A. Neumayr and W. Metzner. Reduction Formula for Fermion Loops and Density Correlations of the 1D Fermi Gas. *Journal of Statistical Physics*, 96(3-4):613–626, 1999.